Accepted Manuscript

Conventional and microwave-assisted synthesis of new 1*H*-benzimidazole-thiazolidinedione derivatives: A potential anticancer scaffold

Pankaj Sharma, T. Srinivasa Reddy, Niggula Praveen Kumar, Kishna Ram Senwar, Suresh K. Bhargava, Nagula Shankaraiah

PII: S0223-5234(17)30481-6

DOI: 10.1016/j.ejmech.2017.06.035

Reference: EJMECH 9530

To appear in: *European Journal of Medicinal Chemistry*

Received Date: 7 May 2017

Revised Date: 20 June 2017

Accepted Date: 21 June 2017

Please cite this article as: P. Sharma, T.S. Reddy, N.P. Kumar, K.R. Senwar, S.K. Bhargava, N. Shankaraiah, Conventional and microwave-assisted synthesis of new 1*H*-benzimidazole-thiazolidinedione derivatives: A potential anticancer scaffold, *European Journal of Medicinal Chemistry* (2017), doi: 10.1016/j.ejmech.2017.06.035.

Graphical Abstract

Conventional and microwave-assisted synthesis of new 1*H*-benzimidazole-thiazolidinedione derivatives: A potential anticancer scaffold

Pankaj Sharma,[a] T. Srinivasa Reddy,[b] Niggula Praveen Kumar,[a] Kishna Ram Senwar,[a] Suresh K. Bhargava,[b]* Nagula Shankaraiah[a]*

[a]*Department of Medicinal Chemistry, National Institute of Pharmaceutical Education and Research (NIPER), Hyderabad 500 037, India*

[b]*Centre for Advanced Materials & Industrial Chemistry (CAMIC), School of Science, RMIT University, GPO BOX 2476, Melbourne-3001, Australia*

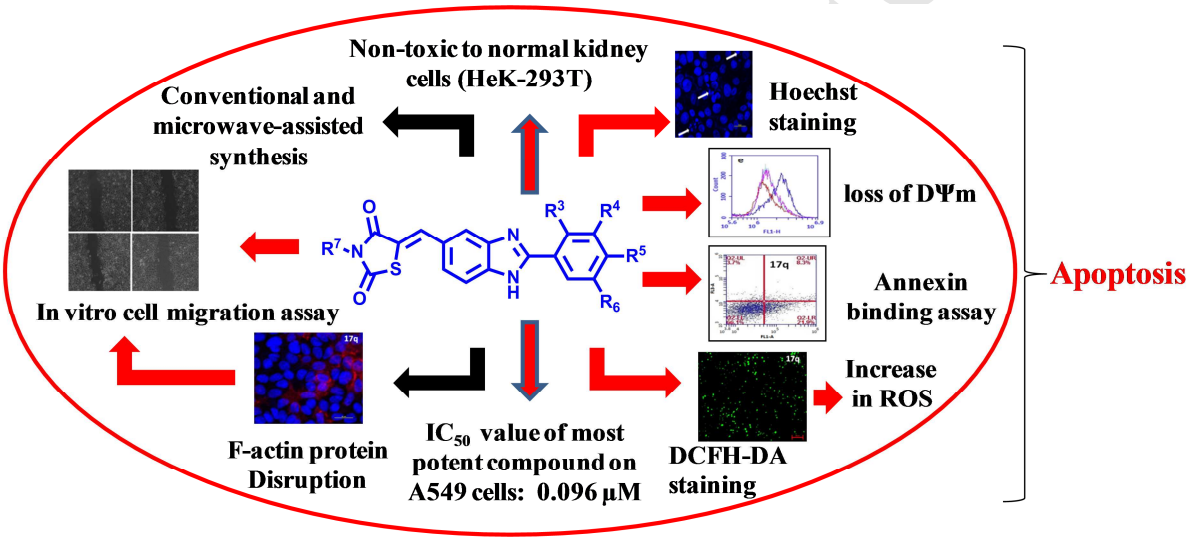

Conventional and microwave-assisted synthesis of new 1*H*-benzimidazole-thiazolidinedione derivatives: A potential anticancer scaffold

Pankaj Sharma,[a] T. Srinivasa Reddy,[b] Niggula Praveen Kumar,[a] Kishna Ram Senwar,[a] Suresh K. Bhargava,[b]* Nagula Shankaraiah[a]*

[a]Department of Medicinal Chemistry, National Institute of Pharmaceutical Education and Research (NIPER), Hyderabad 500 037, India

[b]Centre for Advanced Materials & Industrial Chemistry (CAMIC), School of Science, RMIT University, GPO BOX 2476, Melbourne-3001, Australia

Abstract

A series of new benzimidazole bearing thiazolidinedione derivatives has been designed, synthesized by using conventional as well as microwave-assisted methods. Microwave-assisted synthesis caused a significant reduction in the reaction times and improvement in the yields of all the derivatives. All the new synthesized compounds were evaluated for their *in vitro* cytotoxic potential against selected human cancer cell lines of breast (MDAMB-231), prostate (PC-3), cervical (HeLa), lung (A549) and bone (HT1080) along with a normal kidney cells (HeK-293T). The compounds **17n**, **17p** and **17q** were found to be potent cytotoxic with IC_{50} values in the range of 0.096 to 0.63 µM on PC-3, HeLa, A549 and HT1080 cancer cells. Most of the compounds have found to be safe on normal HeK-293T kidney cells in comparison to cancer cells. The treatment of cells with **17p** and **17q** showed the typical apoptotic morphological features like fragmentation and shrinkage of nuclei. Further, test compounds resulted in inhibition of cell migration through disruption of F-actin protein assembly. Hoechst, DCFH-DA staining, mitochondrial membrane and annexin binding assays revealed that the cancer cell proliferation was inhibited through induction of apoptosis in A549 cells.

Keywords: Benzimidazole, thiazolidinedione, cytotoxicity, apoptosis, microwave.

1. Introduction

In the drug discovery of potential antitumor molecules, significant efforts have been made for the synthesis of new heterocyclic motifs as the main structural design. Such a heterocyclic scaffolds 'benzimidazole' has been recognised as a 'Master Scaffold' considering for their broad spectrum of biological profiles and affinities towards different targets [1,2]. The molecules based on benzimidazole derivatives been reported to have potential anticancer activities against different types of cancers [3,4,5]. Bendamustine [6] and Veliparib [7] are benzimidazole based drugs approved for the cancers treatment. The different substitutions on benzimidazole and its derivatives have been luring researchers throughout the world to investigate their therapeutic potential [8,9,10,11].

On the other hands, thiazolidinedione templates are privileged structural fragments in modern medicinal chemistry and reported to have a diverse range of biological activities [12,13]. The molecules based on this skeleton act as antidiabetic agents *via* peroxisome proliferator-activated receptor-γ (PPAR-γ, pioglitazone and its analogues) [14]. Apart from antidiabetic activity, these scaffolds have shown a broad spectrum of activities such as anti-inflammatory [15], antimicrobial [16], wound-healing [17] *etc*. GSK1059615 (**Figure 1**) is a thiazolidinedione derivative known to exert its anticancer effect through the inhibition of PI3K-α [18]. Liu *et al.* [19] and Jung *et al.* [20] reported thiazolidinediones as potential anticancer agents through inhibition of Raf/MEK/ERK and PI3K/Akt signaling pathways. The research on thiazolidinedione for their anticancer activity has recently gained interest and proven promising for cancer treatment. Furthermore, the different heterocyclic ring systems like pyrrolidine, morpholine, piperidine *etc.* have been recognized as the fundamental building blocks of the most drugs in today's market [21]. These nitrogen-containing heterocycles have the capability to form hydrogen-bonding for selective protein binding and enhanced drug-likeness properties [22]. The significance of these rings are well understood in modern medicinal chemistry and drug discovery, since they are known to play a noteworthy role in molecular properties like three-dimensionality, lipophilicity or polarity, metabolic stability, and toxicity.

<insert figure 1>

In the recent years, microwave assisted synthesis have become a well established tool for the fast assembly of novel chemical entities [23]. The rate of many chemical reactions are increased because of selective absorption of MW energy. The application of microwave

irradiation is the use of catalysts or mineral supported reagents which enables various organic reactions to happen expeditiously at ambient pressure, thus providing unique chemical processes with extraordinary features such as enhanced reaction rates and higher yields [24].

From the past few decades, the amalgamation of two dissimilar chemical entities/pharmacophores with two (or more than two) structural domains having same/different biological functions is being under constant escalation for the exploration of novel and highly active compounds [25,26]. The advantage of using hybridization approach is to turn on different targets by a single molecular entity, thereby increasing therapeutic efficacy and exerting synergistic action with reduced side effects. Hence, in continuation of our research interest [27,28,29] in discovering and developing new potential anticancer agents, we herein designed and synthesized new benzimidazole bearing thiazolidinedione derivatives as potential cytotoxic agents. We have successfully synthesized a series of new derivatives under microwave-assisted technique as well as conventional method using toluene as a solvent with catalytic amounts of piperidine. We have appended the structural features of 2-phenyl-1*H*-benzimidazole to the head-part and various heterocyclic as well as benzyl ring systems like morpholine, piperidine, pyrrolidine, benzyl, 3,4,5-trimethoxybenzyl *etc.* to the tail-part of thiazolidinedione (**Figure 2**). We hypothesized that the synthesized New Chemical Entities (NCEs) could act as potential cytotoxic agents that might act through the induction of apoptosis. In this context, herein we present the synthesis and biological evaluation of new benzimidazole bearing thiazolidinedione derivatives as potential cytotoxic agents and also compared their cytotoxicity profile with a normal kidney cell line.

<insert figure 2>

2. Results and discussion

2.1. Chemistry

The synthetic strategy for thiazolidinediones **2**, **6a–d**, **8a–c**, **10** and new benzimidazole-thiazolidinediones **17a–t** are outlined in **Scheme 1** and **Scheme 2**. The final products **17a–t** were synthesized in a convergent approach by employing Knoevenagel condensation reaction. The reaction of chloroacetic acid (**1**) with thiourea afforded thiazolidinedione **2** (TZD) ring which was subsequently converted into potassium salt of TZD (**3**). On the other

hand, different heterocyclic amines **4a**–**d** were reacted with chloroacetyl chloride to obtain the intermediates **5a**–**d**. The chloroacetylated intermediates **5a**–**d**, benzyl bromides **7a**–**c** and phenacyl bromide **9** were reacted with potassium salt of TZD **3** to obtain different *N*-substituted thiazolidinediones **6a**–**d**, **8a**–**c** and **10**, respectively. Thus, the *N*-substitutions of thiazolidinedione with a variety of heterocyclic amines, benzyl and phenacyl moieties were introduced with different functionalities as well as the scope of diversity.

< **insert Scheme 1**>

Alternatively, 3,4-diaminobenzoic acid (**11**) was converted to its methyl ester **12**, then reacted with different substituted benzaldehydes **13a**–**d** in the presence of sodium metabisulfite to afford 1*H*-benzo[*d*]imidazole-5-carboxylates **14a**–**d**. The ester functionalities in **14a**–**d** were reduced with lithium aluminium hydride to obtain alcohols **15a**–**d** which subsequently were oxidised to their corresponding aldehydes **16a**–**d**. The title compounds **17a**–**t** were accomplished by reacting different thiazolidinediones **2**, **6a**–**d**, **8a**–**c** and **10** with 2-phenyl-1*H*-benzimidazole-5-carbaldehydes **16a**–**d** under Knoevenagel reaction using piperidine in dry toluene. The Knoevenagel condensation reaction for derivatives **17a**–**t** was performed under both conventional as well as microwave-assisted synthesis. Comparative study results obtained by microwave assisted synthesis; versus conventional heating method showed that the conventional heating required more reaction time *i.e.* 5–11 h, however all the reations were completed within 5–10 min. under microwave irradiation technique which caused significant reduction in the reaction times and the yields have been improved from 57–79% (conventional heating) to 74–95% (microwave-assisted reaction) (**Table 1**).

< **insert Scheme 2**>

<insert table 1>

All the synthesized derivatives were characterized by melting point, HRMS (ESI), FT-IR, ^{1}H and ^{13}C NMR techniques. The target model compound **17a** could be easily confirmed by ^{1}H NMR as the aldehydic -CH proton at 10.04 ppm disappeared and a sharp singlet peak of newly formed methine -CH- proton appeared at 7.84 ppm by condensation reaction. All the other aromatic protons of **17a** were found in the range of 7.77–7.36 ppm and methoxy groups appeared as two separate singlets at 4.01 and 3.80 ppm. The examination of ^{13}C NMR spectrum of compound **17a** showed two carbonyl signals at 167.6 and 167.1 ppm. All

other aromatic carbons of **17a** appeared in the range of 153.5–103.9 ppm and aliphatic methoxy carbons at 66.0 and 55.7 ppm. FT-IR spectrum of **17a** showed the carbonyl stretching at 1686 cm^{-1} and -NH- stretching at 3240 cm^{-1}. The ^{1}H and ^{13}C NMR spectra of all other derivatives **17b**–**t** were found almost in a similar pattern like **17a** for their respective aliphatic and aromatic peaks. The HRMS (ESI) of all the final products showed the characteristic $[M + H]^{+}$ molecular ion peaks to their corresponding molecular formula.

2.2. Pharmacology

2.2.1. *In vitro* cytotoxic activity

All the new derivatives of benzimidazole bearing thiazolidinediones **17a**–**t** were evaluated for their *in vitro* cytotoxic potential against selected human cancer cell lines *viz*. breast (MDAMB-231), prostate (PC-3), cervical (HeLa), lung (A549), bone (HT1080) and a normal kidney cells (HeK-293T) using MTT (3-(4,5-dimethylthiazol-2-yl)-2,5-diphenyltetrazolium bromide) reduction assay [10]. The IC_{50} values of **17a**–**t** and reference standard nocodazole have been listed in **Table 2**. It is apparently observed from the primary screening results in **Table 2** that few of the synthesized compounds exhibited potent cytotoxicities below 1.0 µM on tested cancer cell lines. From the close analysis of **Table 2**, compound **17o** was found to be potent cytotoxic with IC_{50} value of 0.27 µM on MDAMB-231 cancer cells. The derivatives **17n**, **17q** and **17t** were found to be active on PC-3 cancer cells with IC_{50} values of 0.63 µM, 0.11 µM and 0.43 µM respectively. Moreover, **17g**, **17l**, **17n**, **17p**, and **17q** displayed the potential cytotoxicities on cervical (HeLa) cancer cell lines with IC_{50}s of 0.51 µM, 0.95 µM, 0.18 µM, 0.32 µM and 0.25 µM respectively. The compounds **17b**, **17g**, **17j**, **17l**, **17m**, **17n**, **17o**, **17p**, **17q**, **17r** and **17t** were found to be active in the range of 0.096 µM–0.98 µM on lung cancer (A549) cell lines which showed the selective cytotoxicity against this cancer cells. Interestingly, **17q** is the highest cytotoxic compound in this series which exhibited IC_{50} value of 0.096 µM, whereas the reference standard displayed IC_{50} of 1.87 µM. Furthermore, **17l**, **17n**, **17o**, **17p**, **17q**, **17r** and **17t** were found to be active on HT1080 (bone cancer) cell lines in the range of 0.16 µM–0.98 µM. It could be noticed from **Table 2** that **17l**, **17m**, **17n** and **17q** showed a broad spectrum of cytotoxic activity on all the examined cancer cells in the range of 0.096 to 4.58 µM.

<insert table 2>

From **Table 2**, it could be observed that compounds **17a**–**d** having free -*N*H functionality produced albeit less active compounds (above 1.0 µM) when compared to *N*-substituted ones (except **17b** on A549 cancer cells). The presence of oxo-ethyl linked heterocyclic rings like morpholine, piperidine, and pyrrolidine produced compounds >1.0 µM with exception of **17g**, **17h** and **17j** which were fairly selective against A549 cancer cells with below IC_{50} of 1.0 µM. Changing the oxo-ethyl linked heterocyclic ring system to benzyl group (**17l**–**q**) produced more active compounds below 1.0 µM on HeLa, A549, and HT1080 cancer cells. One of the compound **17n** containing 3-methyl benzyl moiety at the tail-part of thiazolidinedione was found to be active on all the tested cancer cell lines below 1.78 µM, however, compounds **17o**–**q** having 3,4,5-trimethoxy benzyl substitution at tail-part produced bioactive compounds below 1.0 µM on most of the tested cancer cell lines. On the other hand, substitutions on head-part of thiazolidinedione with benzimidazole containing 3,4,5-trimethoxyphenyl groups generally provided more number of bioactive compounds, however, the most active compound **17q** contained 4-isobutoxy-3-methoxy group on benzimidazole.

These compounds were further evaluated for their *in vitro* cytotoxicity on normal kidney cells (HeK-293T), to find out safety and selectivity against non-cancer cells. It was quite interesting to note that most of the compounds displayed potent cytotoxicity towards cancer cells in comparison to normal HeK-293T kidney cells. It was our keen observation that three of the most active compounds *i.e.* **17n**, **17p** and **17q** were found to be moderately to high selective towards all the tested cancer cell line when compared to normal kidney cells. Compound **17n** displayed IC_{50} values almost 1.9, 5.3, 18.6, 25.8 and 17.6 folds more in MDAMB-231, PC-3, HeLa, A549 and HT1080 respectively when compared to normal HeK-293T cells. Compound **17p** displayed 21.1, 52 and 25.3 times more selectivity in HeLa, A549 and HT1080 cancer cell respectively, however, compound **17q** showed 1.5, 60.5, 26.6, 69.3 and 41.6 times more selectivity in MDAMB-231, PC-3, HeLa, A549 and HT1080 respectively in comparison to normal HeK-293T kidney cells. Based on the cytotoxicity and selectivity of **17p** and **17q** against A549 cells, these were selected for further mechanistic studies of cell growth inhibition.

2.2.2. *In vitro* cell migration assay/Wound healing assay

Migration is a key feature of practically each biological process for the development and maintenance of cells, however it is known to play a major role in tumor progression and

metastatic cascade in cancer cells [30]. Since, cell migration is linked with the metastatic activity of cancer cells, therefore we studied the effect of compounds **17p** and **17q** on A549 cells using *in vitro* cell migration assay/wound healing assay [30]. This assay is based on the observation that, upon creating a new artificial wound, so called "scratch" on a confluent cell monolayer, the cells on the edge of the wound will move toward the opening to close the wound until new cell–cell interactions are established. The treatment of cells with anticancer molecules restricts the migration of cells to close the wound. Henceforth, to test the effect of compounds on cell migration, wounds were created on A549 cell's monolayer by using a 200 µL sterile pipette tip and treated cells with the IC_{50} concentrations of **17p** and **17q** were allowed to migrate into the wounded area. The images of cells to fill-up the wounds were captured at 0, 24 and 48 h after the treatment with the compounds by using phase contrast microscopy. It can be inferred from **Figure 3** that the compounds **17p** and **17q** effectively suppressed the migration of cells into the wounded area, however almost complete healing was observed in DMSO treated control cells after 48 h.

<insert figure 3>

2.2.3. Effect on F-actin polymerisation

Previous report suggested that the migration or motility of cancer cells is an integrated sum of multiple processes triggered by the formation of membrane protrusions or remodelling of cytoskeleton [31]. The cytoskeleton is made-up of various filamentous structures like actin filaments and microtubules. The polymerisation of these actin filaments is considered to be the driving force for the formation of membrane protrusions which help in cancer cell migration as well as stress fibre assembly [32]. It was seen in **Figure 3** that these conjugates inhibited the migration of A549 cancer cells, henceforth it was considered of our interest to examine the effect of these compounds on actin polymerisation and stress fibre formation. The formation of actin cytoskeleton in A549 cells was investigated by using rhodamine phalloidin [33], a red fluorescent dye which binds specifically to F-actin proteins. A549 cancer cells were treated with IC_{50} concentrations of **17p** and **17q** followed by staining with rhodamine-phalloidin. Results from the **Figure 4** clearly demonstrated that the DMSO-treated control A549 cancer cells have a more F-actin extensions however **17p** and **17q** treatment caused the decreased F-actin extensions at the periphery. These results

collectively revealed the ability of these compounds to inhibit the migration potential of A549 cells through disruption of F-actin assembly.

<insert figure 4>

2.2.4. Hoechst staining

Chromatin condensation, DNA fragmentation and nuclear shrinkage are some of the characteristic morphological features of apoptotic cell death. Therefore, we examined the apoptosis-inducing effect of compounds **17p** and **17q** on A549 cancer cells using the Hoechst 33242 nuclear staining method [29]. A549 cancer cells were treated with IC_{50} concentrations of **17p** and **17q**, stained with Hoechst 33242 and observed for nuclear morphological changes under fluorescence microscope. The results from **Figure 5** clearly demonstrated that the nuclear structure of control cells was intact, however **17p** and **17q** treated cells showed the characteristic changes in the morphological features like fragmented and shrinked nuclei (indicated with white arrows) which are typical apoptotic feature.

<insert figure 5>

2.2.5. Effect on intracellular reactive oxygen species (ROS)

Earlier reports suggested that increase in the levels of intracellular reactive oxygen species (ROS) triggers apoptosis induction by altering membrane potential [34,35,36]. We were intrigued by the fact that apoptotic induction in A549 cancer cells could be due to the generation of intracellular ROS, henceforth we tested this possibility by using DCFH-DA (2'-7'-dichlorodihydrofluorescein diacetate) fluorescent dye [37]. DCFH-DA is a non-polar and non-fluorescent dye which gets converted into the highly fluorescent polar derivative DCF when oxidized by intracellular ROS. It could be easily inferred from the **Figure 6** that the DMSO-treated control A549 cells showed less fluorescence, however treatment with IC_{50} concentrations of **17p** and **17q** showed a significant increase in the green fluorescence. This test evidenced the production intracellular ROS, suggesting clearly that these compounds induced apoptosis in A549 cancer cells.

<insert figure 6>

2.2.6. Effect on mitochondrial membrane potential (DΨm)

Mitochondria play an important role in energy metabolism and can also be the source of signals that initiate apoptotic cell death [38]. It has been reported in literature that the loss of mitochondrial membrane potential and increase of intracellular ROS levels are closely connected processes that occur during apoptosis [39]. Henceforth, we examined the effect of **17p** and **17q** on DΨm of A549 cancer cell line by using rhodamine-123 dye [40]. Mitochondria having normal DΨm give a strong green fluorescence; however mitochondrial energization induces the quenching of fluorescence due to less uptake of rhodamine-123, thus causing depolarisation. The change in DΨm can be monitored by shift in the fluorescence intensity by the use of spectrofluorometer. From the **Figure 7a** and **7b** it can be seen the loss of mitochondrial membrane potential of A549 cells. The peak changes from control (DMSO treated) to left (after treatment with IC_{50} concentrations of **17p** and **17q**) as shown in **Figure 7a** indicated depolarisation by the loss of DΨm. The loss in DΨm dropped to 31.6% (**17p**) and 37.3% (**17q**) in comparison to the control. The results from loss of DΨm clearly indicate the induction of apoptosis through the collapse of mitochondrial membrane potential on A549 cells.

<insert figure 7>

2.2.7. Annexin V-FITC/Propidium iodide staining assay

The apoptosis inducing effect of compounds **17p** and **17q** on A549 cancer cells was further investigated using annexin V-FITC/propidium iodide staining assay [41]. This assay facilitate the detection of live cells (Q2-LL; AV-/PI-), early apoptotic cells (Q2-LR; AV+/PI-), late apoptotic cells (Q2-UR; AV+/ PI+) and necrotic cells (Q2-UL; AV-/PI+). A549 cells were treated with IC_{50} concentrations of **17p** and **17q** and stained with annexin V-FITC/propidium iodide. Results from **Figure 8** showed that the percentage of total apoptotic cells (early and late apoptotic cells) increased from 11.4% (control) to 33.8% and 30.2% after treatment with **17p** and **17q** respectively. Therefore, the percentage increase in early and late apoptotic cells clearly indicated that the compound **17p** and **17q** induced apoptosis on A549 cancer cells.

<insert figure 8>

3. Experimental

3.1. Synthesis

3.1.1. Materials and methods

All the reagents, chemicals, starting materials and solvents were procured from commercial sources and were used as such without further purifications. The reactions were monitored by TLC (thin layer chromatography-MERCK silica gel 60-F_{254} pre-coated aluminium plates) under ultra-violet (UV) light. All melting points are uncorrected and were obtained by using Stuart® SMP30 apparatus. All the microwave reactions were performed using monowave 300 instrument (Anton Paar). ^{1}H and ^{13}C NMR were taken on Bruker Avance 500 MHz spectrometer using tetramethylsilane (TMS) as the internal standard and chemical shifts are reported in ppm. Chemical shifts are referenced to TMS (δ 0.00 for ^{1}H NMR and ^{13}C NMR), DMSO-d_6 (δ 2.50 for ^{1}H NMR and 39.5 for ^{13}C NMR) or $CDCl_3$ (δ 7.26 for ^{1}H NMR and 77.15 for ^{13}C NMR). Spin multiplicities are reported as s (singlet), brs (broad singlet), d (doublet), dd (double doublet), t (triplet) and m (multiplet). Coupling constant (*J*) values are reported in hertz (Hz). HRMS were determined with Agilent QTOF mass spectrometer 6540 series instrument and were performed in the ESI techniques at 70 eV. Wherever required, column chromatography was performed using silica gel (100–200 mesh).

*3.1.2. Conventional procedure for the synthesis of benzimidazole-thiazolidinedione (**17a–t**).*

To the suspension of benzimidazole aldehydes (**16a**–**d**, 0.32 mmol), thiazolidinedione (**2**, **6a**–**d**, **8a**–**c** and **10**, 0.35 mmol), in dry toluene (5 mL) was added catalytic amount of piperidine. The reaction mixture was refluxed until complete disappearance of starting materials (5–11 h) was observed by TLC. After cooling, the formed precipitates were filtered, washed with hexane and recrystallized using ethanol to obtain final products **17a**–**t** as yellow solids in 57–79% yields (**table 1**).

*3.1.3. Microwave assisted procedure for the synthesis benzimidazole-thiazolidinedione (**17a–t**).*

A suspension of benzimidazole aldehydes (**16a**–**d**, 0.32 mmol), thiazolidinedione (**2**, **6a**–**d**, **8a**–**c** and **10**, 0.35 mmol), in dry toluene (5 mL) was added catalytic amount of piperidine in a microwave vial (10 mL). The reaction mixture was irradiated at 150 ^{o}C for 5–10 min. After cooling, the formed precipitates were filtered, washed with hexane and recrystallized using ethanol to obtain final products **17a**–**t** as yellow solids in 74–95% yields (**table 1**).

*3.1.3.1. (Z)-5-((2-(3,4,5-Trimethoxyphenyl)-1H-benzo[d]imidazol-5-yl)methylene) thiazolidine-2,4-dione (**17a**)*

Yellow solid; mp: 295–297 °C; FT-IR (cm^{-1}): 3240, 3007, 1735, 1686, 1590, 1291, 1131, 808; ^{1}H NMR (500 MHz, $CDCl_3$+DMSO-d_6): δ 7.83 (s, 1H), 7.69 (s, 1H), 7.61 (d, J = 8.4 Hz, 1H), 7.49–7.47 (m, 2H), 7.34–7.32 (m, 1H), 3.90 (s, 6H), 3.77 (s, 3H); ^{13}C NMR (125 MHz, $CDCl_3$+DMSO-d_6): δ 167.6, 167.1, 153.5, 152.9, 139.2, 133.1, 130.8, 127.6, 126.8, 124.4, 120.4, 122.9, 103.9, 60.0, 55.7; HRMS (ESI): *m/z* calcd for $C_{20}H_{18}N_3O_5S$ 412.0967, found 412.0950 $[M + H]^+$.

*3.1.3.2. (Z)-5-((2-(3,4-Dimethoxyphenyl)-1H-benzo[d]imidazol-5-yl)methylene)thiazolidine-2,4-dione (**17b**)*

Yellow solid; mp: 279–281 °C; FT-IR (cm^{-1}): 3251, 3001, 1728, 1683, 1591, 1285, 1134, 810;; ^{1}H NMR (500 MHz, $CDCl_3$+DMSO-d_6): δ 7.81 (d, J = 14.0 Hz, 1H), 7.73–7.70 (m, 2H), 7.66 (s, 1H), 7.58–7.56 (m, 1H), 7.30 (d, J = 8.4 Hz, 1H), 6.96 (d, J = 8.2 Hz, 1H), 3.90 (s, 3H), 3.85 (s, 3H); (125 MHz, $CDCl_3$+DMSO-d_6): δ 167.7, 167.2, 153.7, 150.3, 148.6, 133.2, 126.5, 124.6, 121.9, 120.1, 119.5, 110.8, 109.6, 55.4, 55.3; HRMS (ESI): *m/z* calcd for $C_{19}H_{16}N_3O_4S$ 382.0862, found 382.0863 $[M + H]^+$.

*3.1.3.3. (Z)-5-((2-(2,4,5-Trimethoxyphenyl)-1H-benzo[d]imidazol-5-yl)methylene) thiazolidine-2,4-dione (**17c**)*

Yellow solid; mp: 278–280 °C; FT-IR (cm^{-1}): 3297, 3145, 2970, 1730, 1685, 1477, 1276, 1035, 798; ^{1}H NMR (500 MHz, $CDCl_3$+DMSO-d_6): δ 7.92 (s, 1H), 7.88 (s, 1H), 7.85 (s, 1H), 7.72 (d, J = 8.4 Hz, 1H), 7.45–7.43 (m, 1H), 6.66 (s, 1H), 4.06 (s, 3H), 3.91 (s, 3H), 3.82 (s, 3H); ^{13}C NMR (125 MHz, DMSO-d_6): δ 168.1, 167.5, 152.2, 151.8, 142.9, 133.5, 126.4, 120.1, 111.9, 108.2, 97.7, 56.3, 55.9, 55.8; HRMS (ESI): *m/z* calcd for $C_{20}H_{18}N_3O_5S$ 412.0967, found 412.0969 $[M + H]^+$.

*3.1.3.4. (Z)-5-((2-(4-Isobutoxy-3-methoxyphenyl)-1H-benzo[d]imidazol-5-yl)methylene) thiazolidine-2,4-dione (**17d**)*

Yellow solid; mp: 290–292 °C; FT-IR (cm^{-1}): 3306, 3160, 2958, 1728, 1683, 1467, 1269, 1022, 796; ^{1}H NMR (500 MHz, DMSO-d_6): δ 7.94 (s, 1H), 7.78–7.69 (m, 4H), 7.44 (d, J = 8.2 Hz, 1H), 7.13 (d, J = 8.5 Hz, 1H), 3.89 (s, 3H), 3.82 (d, J = 6.7 Hz, 2H), 2.09–2.02 (m, 1H), 1.00 (d, J = 6.7 Hz, 6H); ^{13}C NMR (125 MHz, DMSO-d_6): δ 168.1, 167.6, 153.9,

150.2, 149.1, 133.4, 126.8, 124.6, 121.8, 120.4, 119.7, 112.9, 110.1, 74.4, 55.7, 27.7, 19.0; HRMS (ESI): *m/z* calcd for $C_{22}H_{22}N_3O_4S$ 424.1331, found 424.1333 $[M + H]^+$.

*3.1.3.5. (Z)-3-(2-Morpholino-2-oxoethyl)-5-((2-(3,4,5-trimethoxyphenyl)-1H-benzo[d]imidazol-5-yl)methylene)thiazolidine-2,4-dione (**17e**)*

Yellow solid; mp: 198–200 °C; FT-IR (cm^{-1}): 3315, 2991, 1739, 1688, 1649, 1470, 1285, 1022, 819; ^1H NMR (500 MHz, $CDCl_3$+DMSO-d_6): δ 8.00 (s, 1H), 7.76 (s, 1H), 7.65 (d, J = 8.4 Hz, 1H), 7.49 (s, 2H), 7.40 (d, J = 8.5 Hz, 1H), 4.55 (s, 2H), 3.90 (s, 6H), 3.77 (s, 3H), 3.66–3.48 (m, 8H); ^{13}C NMR (125 MHz, $CDCl_3$+DMSO-d_6): δ 166.9, 165.1, 163.0, 153.6, 152.4, 139.2, 134.7, 131.6, 128.5, 126.7, 124.8, 124.4, 117.9, 103.9, 65.8, 65.7, 60.0, 55.7, 44.4, 42.0, 41.8; HRMS (ESI): *m/z* calcd for $C_{26}H_{27}N_4O_7S$ 539.1600, found 539.1594 $[M + H]^+$.

*3.1.3.6. (Z)-5-((2-(3,4-Dimethoxyphenyl)-1H-benzo[d]imidazol-5-yl)methylene)-3-(2-morpholino-2-oxoethyl)thiazolidine-2,4-dione (**17f**)*

Yellow solid; mp: 268–270 °C; FT-IR (cm^{-1}): 3210, 2987, 1736, 1682, 1600, 1440, 1266, 807; ^1H NMR (500 MHz, $CDCl_3$+DMSO-d_6): δ 8.19 (s, 1H), 7.93–7.72 (m, 4H), 7.50 (d, J = 8.2 Hz, 1H), 7.16 (d, J = 8.4 Hz, 1H), 4.61 (s, 2H), 3.89 (s, 3H), 3.84 (s, 3H), 3.64–3.44 (m, 8H); ^{13}C NMR (125 MHz, $CDCl_3$+DMSO-d_6): δ 166.9, 165.2, 163.1, 153.7, 150.6, 148.7, 134.8, 126.5, 124.7, 121.6, 191.7, 117.7, 11.3, 109.8, 65.8, 55.4, 55.3, 44.4, 42.1, 41.8; HRMS (ESI): *m/z* calcd for $C_{25}H_{25}N_4O_6S$ 509.1495, found 509.1497 $[M + H]^+$.

*3.1.3.7. (Z)-3-(2-Morpholino-2-oxoethyl)-5-((2-(2,4,5-trimethoxyphenyl)-1H-benzo[d]imidazol-5-yl)methylene)thiazolidine-2,4-dione (**17g**)*

Yellow solid; mp: 303–305 °C; FT-IR (cm^{-1}): 3312, 2980, 1741, 1685, 1651, 1453, 1282, 1023, 805; ^1H NMR (500 MHz, $CDCl_3$+DMSO-d_6): δ 8.03 (s, 1H), 7.91–7.89 (m, 2H), 7.76 (d, J = 8.4 Hz, 1H), 7.46–7.44 (m, 1H), 6.80 (s, 1H), 4.62 (s, 2H), 4.10 (s, 3H), 3.96 (s, 3H), 3.90 (s, 3H), 3.70–3.52 (m, 8H, merged with DMSO-moisture); ^{13}C NMR (125 MHz, $CDCl_3$+DMSO-d_6): δ 167.0, 165.2, 163.1, 152.2, 151.8, 151.5, 142.8, 134.9, 126.2, 125.0, 117.4, 112.0, 108.0, 97.2, 65.8, 56.1, 55.8, 55.7, 44.4, 42.1, 41.8; HRMS (ESI): *m/z* calcd for $C_{26}H_{27}N_4O_7S$ 539.1600, found 539.1606 $[M + H]^+$.

*3.1.3.8. (Z)-3-(2-Oxo-2-(piperidin-1-yl)ethyl)-5-((2-(3,4,5-trimethoxyphenyl)-1H-benzo[d]imidazol-5-yl)methylene)thiazolidine-2,4-dione (**17h**)*

Yellow solid; mp: 180–182 °C; FT-IR (cm^{-1}): 3250, 2955, 1730, 1677, 1630, 1285, 1230, 813; ^{1}H NMR (500 MHz, DMSO-d_6): δ 7.69 (s, 1H), 7.49 (s, 1H), 7.40–7.38 (m, 3H), 7.05 (d, J = 8.1 Hz, 1H), 4.57 (s, 2H), 3.90 (d, J = 8.5 Hz, 9H), 3.63 (t, J = 5.3 Hz, 2H), 3.52–3.48 (m, 2H), 1.73–1.69 (m, 4H), 1.65–1.55 (m, 2H); ^{13}C NMR (125 MHz, $CDCl_3$+DMSO-d_6): δ 167.4, 165.5, 162.1, 152.9, 153.6, 139.4, 134.9, 126.9, 125.1, 124.0, 118.0, 103.8, 60.3, 55.7, 45.2, 42.8, 41.7, 25.5, 24.6, 23.6; HRMS (ESI): *m/z* calcd for $C_{27}H_{29}N_4O_6S$ 537.1808, found 537.1808 $[M + H]^+$.

*3.1.3.9. (Z)-3-(2-Oxo-2-(piperidin-1-yl)ethyl)-5-((2-(2,4,5-trimethoxyphenyl)-1H-benzo[d]imidazol-5-yl)methylene)thiazolidine-2,4-dione (**17i**)*

Yellow solid; mp: 265–267 °C; FT-IR (cm^{-1}): 3249, 2967, 1732, 1677, 1626, 1406, 1287, 1245, 998, 815; ^{1}H NMR (500 MHz, $CDCl_3$+DMSO-d_6): δ 7.94 (s, 1H), 7.89–7.86 (m, 1H), 7.78 (s, 1H), 7.66–7.63 (m, 1H), 7.33, (d, J = 8.5 Hz, 1H), 6.68 (s, 1H), 4.48 (s, 2H), 4.03 (s, 3H), 3.90 (s, 3H), 3.85 (s, 3H), 3.45–3.42 (m, 4H), 1.60–1.48 (m, 6H); ^{13}C NMR (125 MHz, $CDCl_3$+DMSO-d_6): δ 167.0, 165.2, 162.2, 152.1, 151.7, 151.5, 142.8, 134.7, 128.4, 127.6, 126.2, 124.9, 117.5, 115.5, 111.9, 108.0, 96.7, 55.9, 55.8, 55.6, 45.1, 42.6, 42.0, 25.6, 24.8, 23.6; HRMS (ESI): *m/z* calcd for $C_{27}H_{29}N_4O_6S$ 537.1808, found 537.1798 $[M + H]^+$.

*3.1.3.10. (Z)-3-(2-Oxo-2-(pyrrolidin-1-yl)ethyl)-5-((2-(3,4,5-trimethoxyphenyl)-1H-benzo[d]imidazol-5-yl)methylene)thiazolidine-2,4-dione (**17j**)*

Yellow solid; mp: 269–271 °C; FT-IR (cm^{-1}): 3241, 2988, 1735, 1670, 1632, 1290, 1255, 813; ^{1}H NMR (500 MHz, $CDCl_3$+DMSO-d_6): δ 8.12 (s, 1H), 7.88–7.49 (m, 2H), 7.55–7.50 (m, 3H), 4.48 (s, 2H), 3.91 (s, 6H), 3.74 (s, 3H), 3.53 (t, J = 6.7 Hz, 2H), 3.30 (t, J = 6.9 Hz, 2H), 1.95–1.89 (m, 2H), 1.82–1.77 (m, 2H); ^{13}C NMR (125 MHz, $CDCl_3$+DMSO-d_6): δ 167.1, 165.3, 162.7, 153.7, 153.2, 139.3, 140.0, 128.8, 128.1, 126.8, 125.2, 124.7, 118.0, 104.0, 60.1, 56.0, 45.8, 45.0, 43.1, 25.2, 23.6; HRMS (ESI): *m/z* calcd for $C_{26}H_{27}N_4O_6S$ 523.1651, found 523.1662 $[M + H]^+$.

*3.1.3.11. (Z)-3-(2-(2,6-Dimethylmorpholino)-2-oxoethyl)-5-((2-(4-isobutoxy-3-methoxy phenyl)-1H-benzo[d]imidazol-5-yl)methylene)thiazolidine-2,4-dione (**17k**)*

Yellow solid; mp: 302–304 °C; FT-IR (cm^{-1}): 3234, 2978, 1737, 1683, 1631, 1442, 1259, 1082, 1019, 809; ^{1}H NMR (500 MHz, DMSO-d_6): δ 8.11 (s, 1H), 7.93–7.71 (m, 4H), 7.50 (d, J = 8.2 Hz, 1H), 7.14 (d, J = 8.2 Hz, 1H), 4.79 (d, J = 16.6 Hz, 1H), 4.50 (d, J = 16.6 Hz, 1H), 4.15 (d, J = 12.7 Hz, 1H), 3.89–3.81 (m, 6H), 3.58–3.44 (m, 2H), 2.79 (t, J = 11.4 Hz,

1H), 2.33 (t, *J* = 11.7 Hz, 1H), 2.08–2.03 (m, 1H), 1.13–1.08 (m, 6H), 1.00 (d, *J* = 6.4 Hz, 6H); ^{13}C NMR (125 MHz, DMSO-d_6): δ 167.2, 165.4, 163.1, 150.3, 149.1, 135.1, 126.6, 124.7, 121.8, 119.8, 117.7, 112.9, 110.1, 74.5, 71.3, 71.0, 55.7, 49.3, 46.8, 42.6, 27.7, 19.0, 18.6, 18.3; HRMS (ESI): *m/z* calcd for $C_{30}H_{35}N_4O_6S$ 579.2277, found 579.2284 $[M + H]^+$.

*3.1.3.12. (Z)-3-Benzyl-5-((2-(3,4,5-trimethoxyphenyl)-1H-benzo[d]imidazol-5-yl)methylene) thiazolidine-2,4-dione (**17l**)*

Yellow solid; mp: 263–265 °C; FT-IR (cm^{-1}): 3428, 3010, 2967, 1735, 1670, 1357, 1275, 1211, 1021, 777; ^{1}H NMR (500 MHz, $CDCl_3$+DMSO-d_6): δ 8.06 (s, 1H), 7.84–7.81 (m, 2H), 7.73 (d, *J* = 8.4 Hz, 1H), 7.59 (s, 2H), 7.47 (d, *J* = 8.5 Hz, 1H), 7.39–7.28 (m, 4H), 4.90 (s, 2H), 3.98 (s, 6H), 3.87 (s, 3H); ^{13}C NMR (125 MHz, $CDCl_3$+DMSO-d_6): δ 167.1, 165.4, 153.8, 153.0, 139.3, 135.3, 135.1, 134.9, 128.3, 127.6, 124.6, 117.8, 113.2, 104.0, 103.9, 59.9, 55.8, 44.4; HRMS (ESI): *m/z* calcd for $C_{27}H_{24}N_3O_5S$ 502.1437, found 502.1435 $[M + H]^+$.

*3.1.3.13. (Z)-3-(3-Methylbenzyl)-5-((2-(3,4,5-trimethoxyphenyl)-1H-benzo[d]imidazol-5-yl)methylene)thiazolidine-2,4-dione (**17m**)*

Yellow solid; mp: 235–237 °C; FT-IR (cm^{-1}): 3349, 2967, 1733, 1655, 1352, 1129, 1001, 744; ^{1}H NMR (500 MHz, $CDCl_3$+DMSO-d_6): δ 8.13 (s, 1H), 7.86 (s, 1H,), 7.74 (d, *J* = 8.4 Hz, 1H), 7.55 (s, 2H,), 7.49 (d, *J* = 9.5 Hz, 1H), 7.24 (t, *J* = 7.6 Hz, 1H), 7.13–7.09 (m, 3H), 4.80 (s, 2H), 3.90 (s, 6H), 3.74 (s, 3H), 2.28 (s, 3H); ^{13}C NMR (125 MHz, DMSO-d_6): δ 167.3, 165.5, 153.7, 153.2, 139.3, 137.8, 135.4, 135.0, 128.8, 128.5, 128.3, 128.0, 126.8, 124.8, 124.7, 124.6, 118.0, 104.0, 60.1, 56.0, 44.5, 20.9; HRMS (ESI): *m/z* calcd for $C_{28}H_{26}N_3O_5S$ 516.1593, found 516.1598 $[M + H]^+$.

*3.1.3.14. (Z)-3-(3-Methylbenzyl)-5-((2-(2,4,5-trimethoxyphenyl)-1H-benzo[d]imidazol-5-yl)methylene)thiazolidine-2,4-dione (**17n**)*

Yellow solid; mp: 197–199 °C; FT-IR (cm^{-1}): 3422, 3002, 2942, 1734, 1678, 1375, 1278, 1206, 1027, 778; ^{1}H NMR (500 MHz, $CDCl_3$+DMSO-d_6): δ 7.96 (s, 1H), 7.92 (s, 1H), 7.78 (s, 1H), 7.67 (d, *J* = 8.3 Hz, 1H), 7.33 (d, *J* = 8.4 Hz, 1H), 7.16-7.10 (m, 3H), 7.03 (d, *J* = 7.0 Hz, 1H), 6.63 (s, 1H), 4.78 (s, 2H), 4.03 (s, 3H), 3.90 (s, 3H), 3.89 (s, 3H), 2,26 (s, 3H); ^{13}C NMR (125 MHz, $CDCl_3$+DMSO-d_6): δ 167.1, 165.4, 152.2, 151.8, 151.1, 142.8, 137.5, 134.8, 134.7, 128.3, 128.2, 128.0, 126.4, 125.0, 124.7, 117.6, 115.4, 111.8, 107.6, 96.6,

55.9, 55.6, 44.3, 20.7; HRMS (ESI): *m/z* calcd for $C_{28}H_{26}N_3O_5S$ 516.1593, found 516.1591 $[M + H]^+$.

*3.1.3.15. (Z)-3-(3,4,5-Trimethoxybenzyl)-5-((2-(3,4,5-trimethoxyphenyl)-1H-benzo[d] imidazol-5-yl)methylene)thiazolidine-2,4-dione (**17o**)*

Yellow solid; mp: 134–136 °C; FT-IR (cm^{-1}): 3351, 2997, 1727, 1662, 1580, 1120, 815, 795, 617; ^1H NMR (500 MHz, $CDCl_3$): δ 8.01 (s, 1H), 7.86–7.52 (m, 2H), 7.41–7.36 (m, 3H), 6.71 (s, 2H), 4.82 (s, 2H), 3.91 (s, 3H), 3.85–3.83 (m, 15H); ^{13}C NMR (125 MHz, $CDCl_3$): δ 168.3, 166.4, 154.0, 153.4, 140.8, 138.0, 135.3, 131.1, 128.3, 126.4, 124.6, 119.5, 106.4, 104.3, 61.2, 61.0, 56.4, 56.3, 45.7; HRMS (ESI): *m/z* calcd for $C_{30}H_{30}N_3O_8S$ 592.1754, found 592.1757 $[M + H]^+$.

*3.1.3.16. (Z)-5-((2-(3,4-Dimethoxyphenyl)-1H-benzo[d]imidazol-5-yl)methylene)-3-(3,4,5-trimethoxybenzyl)thiazolidine-2,4-dione (**17p**)*

Yellow solid; mp: 246–248 °C; FT-IR (cm^{-1}): 3334, 3001, 1729, 1663, 1586, 1126,798, 615; ^1H NMR (500 MHz, DMSO-d_6): δ 8.12 (s, 1H), 7.90–7.64 (m, 4H), 7.48 (d. J = 8.2 Hz, 1H), 7.15 (d, J = 8.9 Hz, 1H), 6.62 (s, 2H), 4.77 (s, 2H), 3.88 (s, 3H), 3.84 (s, 3H), 3.74 (s, 6H), 3.62 (s, 3H); ^{13}C NMR (125 MHz, DMSO-d_6): δ 167.5, 165.7, 152.9, 150.7, 148.9, 137.1, 135.0, 131.1, 128.8, 128.2, 126.7, 121.9, 119.7, 117.9, 111.8, 109.8, 105.2, 59.9, 56.0, 55.8, 55.5, 44.8; HRMS (ESI): *m/z* calcd for $C_{29}H_{28}N_3O_7S$ 562.1648, found 562.1635 $[M + H]^+$.

*3.1.3.17. (Z)-5-((2-(4-Isobutoxy-3-methoxyphenyl)-1H-benzo[d]imidazol-5-yl)methylene)-3-(3,4,5-trimethoxybenzyl)thiazolidine-2,4-dione (**17q**)*

Yellow solid; mp: 298–300 °C; FT-IR (cm^{-1}): 3342, 2960, 1670, 1594, 1462, 1220, 1126, 800; ^1H NMR (500 MHz, $CDCl_3$): δ 7.97 (s, 1H), 7.75 (s, 1H), 7.70–7.68 (m, 1H), 7.61 (d, J = 8.1 Hz, 1H), 7.48 (s, 1H), 7.33 (d, J = 8.1 Hz, 1H), 6.91 (d, J = 8.3 Hz, 1H), 6.61–6.56 (m, 2H), 4.74 (s, 2H), 3.90 (s, 3H), 3.77–3.70 (m, 11H), 2.14–2.06 (m, 1H), 0.98 (d, J = 6.3 Hz, 6H); ^{13}C NMR (125 MHz, $CDCl_3$): δ 168.3, 166.4, 153.4, 151.4, 150.1, 137.9, 135.5, 131.1, 127.9, 126.2, 121.7, 119.8, 119.0, 112.9, 110.5, 106.4, 75.6, 61.0, 56.3, 56.2, 45.6, 28.2, 19.4; HRMS (ESI): *m/z* calcd for $C_{32}H_{34}N_3O_7S$ 604.2117, found 604.2121 $[M + H]^+$.

*3.1.3.18. (Z)-3-(2-Oxo-2-phenylethyl)-5-((2-(3,4,5-trimethoxyphenyl)-1H-benzo[d]imidazol-5-yl)methylene)thiazolidine-2,4-dione (**17r**)*

Yellow solid; mp: 183–185 °C; FT-IR (cm^{-1}): 3331, 2967, 1745, 1670, 1576, 1456, 1240, 1016, 814; ^{1}H NMR (500 MHz, $CDCl_3$+DMSO-d_6): δ 8.01 (s, 1H), 7.97 (d, J = 8.4 Hz, 2H,), 7.78 (s, 1H), 7.70 (d, J = 8.4 Hz, 1H,), 7.61 (t, J = 7.5 Hz, 1H,), 7.55 (s, 2H), 7.50–7.47 (m, 2H), 7.42–7.40 (m, 1H), 5.16 (s, 2H), 3.94 (s, 6H), 3.84 (s, 3H); ^{13}C NMR (125 MHz, $CDCl_3$+DMSO-d_6): δ 190.0, 166.7, 165.0, 153.5, 152.9, 143.0, 139.3, 134.9, 133.8, 133.5, 128.5, 127.7, 126.7, 125.0, 124.0, 117.8, 113.9, 103.9, 60.0, 55.7, 47.2; HRMS (ESI): *m/z* calcd for $C_{28}H_{24}N_3O_6S$ 530.1386, found 530.1384 $[M + H]^+$.

3.1.3.19. (Z)-3-(2-Oxo-2-phenylethyl)-5-((2-(2,4,5-trimethoxyphenyl)-1H-benzo[d]imidazol-5-yl)methylene)thiazolidine-2,4-dione ***(17s)***

Yellow solid; mp: 264–266 °C; FT-IR (cm^{-1}): 3346, 2942, 1732, 1678, 1585, 1450, 1226, 1027, 813; ^{1}H NMR (500 MHz, $CDCl_3$+DMSO-d_6): δ 7.98–7.97 (m, 3H), 7.90 (s, 1H), 7.80 (s, 1H), 7.66–7.61 (m, 2H), 7.49 (d, J = 7.6 Hz, 2H), 7.36 (d, J = 8.2 Hz, 1H), 6.67 (s, 1H), 5.16 (s, 2H), 4.04 (s, 3H), 3.90 (s, 3H), 3.86 (s, 3H); ^{13}C NMR (125 MHz, $CDCl_3$+DMSO-d_6): δ 189.9, 166.9, 165.1, 152.1, 151.7, 151.6, 142.8, 135.2, 133.7, 133.5, 128.4, 127.6, 126.1, 125.0, 117.3, 115.9, 111.9, 107.9, 96.6, 55.9, 55.6, 47.0; HRMS (ESI): *m/z* calcd for $C_{28}H_{24}N_3O_6S$ 530.1386, found 530.1391$[M + H]^+$.

3.1.3.20. (Z)-5-((2-(3,4-Dimethoxyphenyl)-1H-benzo[d]imidazol-5-yl)methylene)-3-(2-oxo-2-phenylethyl)thiazolidine-2,4-dione ***(17t)***

Yellow solid; mp: 237–239 °C; FT-IR (cm^{-1}): 3350, 2957, 1735, 1667, 1578, 1470, 1220, 1007, 815; ^{1}H NMR (500 MHz, $CDCl_3$+DMSO-d_6): δ 8.11 (s, 1H), 8.08 (d, J = 7.2 Hz, 2H), 7.84 (s, 1H), 7.80–7.78 (m, 2H), 7.73–7.68 (m, 2H), 7.59–7.56 (m, 2H), 7.48–7.46 (m, 1H), 7.11 (d, J = 8.4 Hz, 1H), 5.28 (s, 2H), 3.92 (s, 3H), 3.87 (s, 3H); ^{13}C NMR (125 MHz, $CDCl_3$+DMSO-d_6): δ 190.7, 166.9, 165.1, 153.8, 150.7, 148.7, 135.2, 134.0, 133.6, 128.7, 128.0, 126.5, 124.8, 121.5, 119.8, 117.6, 111.4, 109.8, 55.4, 47.5; HRMS (ESI): *m/z* calcd for $C_{27}H_{22}N_3O_5S$ 500.1280, found 500.1280 $[M + H]^+$.

3.2. Biological assays

3.2.1. Cell cultures

Breast (MDAMB-231), prostate (PC-3), cervical (HeLa), lung (A549), bone (HT1080) and normal kidney cells (HeK-293T) were procured from ATCC (American Type Cell Culture Collection), Maryland, USA and were grown in suitable MEM (Minimum Essential

Medium, Sigma) or DMEM (Dulbecco Modified Eagle medium, Sigma) with supplement of 10% fetal bovine serum stabilized with 1X antibiotic-antimycotic solution (Sigma) in a CO_2 incubator with 5% CO_2 and 90% relative humidity at 37 °C. When the confluency of cells reached upto 80-90%, were treated with 0.25 % trypsin/1 mM EDTA solution for further passage.

3.2.2. MTT (3-(4,5-dimethylthiazol-2-yl)-2,5-diphenyltetrazolium bromide) assay

The cytotoxic potential of compounds **17a**–**t** was examined using MTT reduction assay. 1×10^4 cells/well were seeded in 96-well plates in 100 µL DMEM, supplemented with 10% FBS in each well and incubated in CO_2 incubator for 24 h at 37 °C. The medium was replaced with culture medium containing test compounds dissolved in DMSO (Dimethyl sulfoxide). Wells having only DMSO were used as the control. After incubating for 48 h, 10 µL of MTT was added to each well and further incubated for 4 hour in dark at 37 °C. After 4 h of incubation period, the MTT media was removed and DMSO (100 µL) was put into each well to dissolve the crystallized formazan product. The absorbance was recorded on a micro-plate reader at 570 nm wavelength and at a reference wavelength of 630 nm. The percentage inhibition was calculated as 100–[(Mean OD of treated cell × 100)/Mean OD of vehicle treated cells (DMSO)]. All the experiments were performed at least three independent experiments and IC_{50} values were computed by using Probit Software.

3.2.3. *In vitro* cell migration assay/Wound healing assay

A549 cells (5×10^5 cells/well) were grown as confluent monolayers for 24 h in six well plate. Then artificial wound/scratch were created on cell monolayers using 200 µL sterile tip of pipette and non-adherent cells were removed by washing twice with PBS (Phosphate-buffered saline). The media containing IC_{50} concentrations of compounds **17p** and **17q** were added to each well and the wells without compound were shown as Control. The movement/migration of cells across the wounded/scratched area was photographed by using Nikon phase contrast microscope immediately at 0 h, 24 h and 48 h of time interval subsequent to treatment in three or more randomly selected fields.

3.2.4. F-actin staining

A549 cancer cells (1×10^6 cells/well) were grown on cover slips for 24 h in 6 well plate and incubated with IC_{50} concentrations of compound **17p** and **17q** for 24 h. After compounds treatment, the cells were washing with PBS and fixed with 4% *para*-formaldehyde solution.

Cells were incubated with rhodamine-phalloidin (red fluorescent dye) for staining of F-actin and with Hoechst 33242 for nuclear staining. Then cells were washed thrice with PBS and mounted with ProLong Gold anti-fade reagent (Molecular Probes, Eugene, OR) on microscopic slide and visualized by microscopy (Nikon). The fluorescent images were captured by using 20X magnification lenses.

3.2.5. Hoechst nuclear staining

A549 lung cancer cells (5×10^4 cells/well) were cultured on coverslips in a 6 wells plate and permitted to adhere for 24 h. The culture medium containing IC_{50} concentrations of compound **17p** and **17q** were added to them. After incubation for 24 h, culture medium was separated; cells were washed and fixed with 4% *para*-formaldehyde solution for 10 min at 4 °C. Cells were washed two times with PBS and stained with Hoechst 33242 (5 µg/ mL) at room temperature for 30 min. The excess dye was separated by washing cells two times with PBS and suspension of cells was mounted on slides and examined for change in the morphology under fluorescence microscopy at an absorbance of 350 nm for excitation and 460 nm for emission (Nikon, magnification 40x).

3.2.6. Measurement of reactive oxygen species (ROS) levels

Intracellular ROS levels in A549 cancer cells were assessed by using DCFH-DA (2'-7'-dichlorodihydrofluorescein diacetate). A549 cells (5×10^5 cells/mL) were plated in 6 wells plate and were allowed to grow overnight. The cells were incubated for 24 h with IC_{50} concentrations of **17p** and **17q**. After treatment with compounds, the media was replaced with DCFH-DA (10 µM) containing culture medium followed by incubation for 30 minutes at room temperature in dark. Cells (5×10^4 cells/mL) were washed with PBS, collected from well-plate and suspended again in PBS. The fluorescence intensity of the DCF (2', 7'-dichlorofluorescein produced by the hydrolysis of DCFH-DA from each sample was analyzed by spectrofluorometer at an excitation of 488 nm and emission wavelength 525 nm. Fluorescent images were captured by using Nikon ECLIPSETE2000-S fluorescence microscope.

3.2.7. Measurement of Mitochondrial Membrane Potential (DΨm)

A549 cells (5×10^5 cells/mL) were cultured in 6 well plates and allowed to adhere overnight. The cells were treated with IC_{50} concentrations of **17p** and **17q** for 24 h. After 24 h of treatment, the adherent cells were collected by trypsinisation, washed with PBS (500

µL) and suspended in a solution of PBS containing rhodamine-123 (10 µg/mL) and additionally incubated at room temperature for 30 minutes. Cells were washed two times with PBS to remove excess dye and resuspended in PBS. The samples were analyzed for fluorescence using spectrofluorometer.

3.2.8. Annexin V-FITC/propidium iodide dual staining assay

To quantify the percentage of apoptotic cells, annexin V-FITC/propidium iodide dual staining assay was performed using A549 cells. Cells (10^6/mL per well) were seeded in six-well plates and allowed to grow for 24 h. After treatment with IC_{50} concentrations of **17p** and **17q** for 24 h, cells were collected by trypsinisation. The collected cells were then washed two times with ice-cold PBS, then incubated with 200 µL1 × binding buffer containing 5 µL Annexin V-FITC, and then in 300 µL1 × binding buffer containing 5 µL Propidium iodide (PI) at room temperature in the dark for 5 min and incubate for 15 min. After 15 min of the incubation period, cells were analysed for a percentage of apoptosis using BD-C6 accuri flow-cytometer.

4. Conclusion

In conclusion, a series of new benzimidazole-containing thiazolidinedione derivatives was synthesized by using conventional as well as microwave-assisted technique and evaluated for their *in vitro* cytotoxic activity against different human cancer cell lines *viz.* MDAMB-231, PC-3, HeLa, A549, HT1080 and a normal kidney cell (HeK-293T). Some of the synthesized compounds were found to be more potent with IC_{50} values ranging from 0.096 to 0.98 µM. Apart from this, a number of compounds were found to be active against A549 cancer cells below 1.0 µM in comparison to others tested cancer cells. The cytotoxic profiles on normal HeK-293T cells revealed that most of these compounds were more selective towards the cancer cells when compared to normal cells. The exposure of A549 lung cancer cells to **17p** and **17q** resulted in remarkable inhibition of cell migration through disruption of F-actin assembly. The apoptosis inducing effect of the compounds were studied by different techniques like Hoechst 33242 nuclear staining, DCFH-DA, rhodamine-123, and annexin V-FITC/propidium iodide staining. Moreover, **17p** and **17q** treatment led to the collapse of the mitochondrial membrane potential (DΨm) and increased levels of reactive oxygen species (ROS) in A549 cells. Overall, the different studies suggested that these new compounds have the potential to be developed as cytotoxic agents

and their structural modifications could lead to the generation of promising anticancer agents.

Acknowledgements

P.S. is thankful to DoP, Ministry of Chemicals & Fertilizers, Govt. of India, for the award of NIPER fellowship. Dr. N. Shankaraiah gratefully acknowledges SERB, DST, Govt. of India for research grant (YSS-2015-001709).

References

1. G. Yadav, S. Ganguly,. Eur. J. Med. Chem. 97 (2015) 419–443.
2. (a) W. Akhtar, M.F. Khan, G. Verma, M. Shaquiquzzaman, M.A. Rizvi, S.H. Mehdi, M. Akhter, M.M. Alam, Eur. J. Med. Chem. 126 (2017) 705–753; (b) A. Kamal, S. Nekkanti, N. Shankaraiah, S. Manda. Drug Resistance in Bacteria, Fungi, Malaria, and Cancer; Springer International Publishing, 2017, pp. 609–629.
3. W. Gu, T.-T. Miao, D.-W. Hua, X.-Y. Jin, X.-B. Tao, C.-B. Huang, S.-F. Wang, Bioorg. Med. Chem. Lett. 27 (2017) 1296–1300.
4. M.K. Kim, H. Shin, K.S. Park, H. Kim, J. Park, K. Kim, J. Nam, H. Choo, Y. Chong, J. Med. Chem. 58 (2015) 7596–7602.
5. P. Sharma, T.S. Reddy, D. Thummuri, K.R. Senwar, N.P. Kumar, V.G.M. Naidu, S.K. Bhargava, N. Shankaraiah, Eur. J. Med. Chem. 124 (2016) 608–621.
6. R. Kath, K. Blumenstengel, H.J. Fricke, K. Höffken, J. Cancer Res. Clin. Oncol. 127 (2001) 48–54.
7. L.M. Wagner, Onco. Targets Ther. 8 (2015) 1931–1939.
8. (a) G. Chen, Z. Liu, Y. Zhang, X. Shan, L. Jiang, Y. Zhao, W. He, Z. Feng, S. Yang, G. Liang, ACS Med. Chem. Lett. 4 (2013) 69–74; (b) A. Kamal, P. Suresh, M.J.P. Ramaiah, T.S. Reddy, R.K. Kapavarapu, S. Imthiajali, T.L.N. Reddy, S.N.C.V.L. Pushpavalli, N. Shankaraiah, M.-P. Bhadra, Bioorg. Med. Chem. 21 (2013) 5198–5208; (c) A. Kamal, T.S. Reddy, M.V.P.S. Vishnuvardhan, V.K. Nimbarte, A.V.S. Rao, V. Srinivasulu, N. Shankaraiah, Bioorg. Med. Chem. 23 (2015) 4608–4623.
9. I. Khan, M.A. Tantray, H. Hamid, M.S. Alam, A. Kalam, A. Dhulap, Bioorg. Med. Chem. Lett. 26 (2016) 4020–4024.
10. T.S. Reddy, H. Kulhari, V.G. Reddy, V. Bansal, A. Kamal, R. Shukla, Eur. J. Med. Chem. 101 (2015) 790–805.

11. P. Sharma, D. Thummuri, T.S. Reddy, K.R. Senwar, V.G.M. Naidu, G. Srinivasulu, S.K. Bharghava, N. Shankaraiah, Eur. J. Med. Chem. 122 (2016) 584–600.
12. D. Panigrahy, L.Q. Shen, M.W. Kieran, A. Kaipainen, Expert Opin. Investig. Drugs 12 (2003) 1925–1937.
13. V.S. Jain, D.K. Vora, C.S. Ramaa, Bioorg. Med. Chem. 21 (2013) 1599–1620.
14. A. Pfützner, M. M. Weber, T. Forst, Expert Opin. Pharmacother. 8 (2007) 1985–1998.
15. L.A. Faine, M. Rudnicki, F.A. César, B.L. Heras, L. Boscá, E.S. Souza, M.Z. Hernandes, S.L. Galdino, M.C. Lima, I.R. Pitta, D.S. Abdalla, Curr. Med. Chem. 18 (2011) 3351–3360.
16. M. Guo, C.-J. Zheng, M.-X. Song, Y. Wu, L.-P. Sun, Y.-J. Li, Y. Liu, H.-R. Piao, Bioorg. Med. Chem. Lett. 23 (2013) 4358–4361.
17. Y. Wu, S. Karna, C.H. Choi, M. Tong, H.-H. Tai, D.H. Na, C.H. Jang, H. Cho, J. Med. Chem. 54 (2011) 5260–5264.
18. S.D. Knight, N.D. Adams, J.L. Burgess, A.M. Chaudhari, M.G. Darcy, C.A. Donatelli, J.I. Luengo, K.A. Newlander, C.A. Parrish, L.H. Ridgers, M,A. Sarpong, S.J. Schmidt, G.S. Van Aller, J.D. Carson, M.A. Diamond, P.A. Elkins, C.M. Gardiner, E. Garver, S.A. Gilbert, R.R. Gontarek, J.R. Jackson, K.L. Kershner, L. Luo, K. Raha, C.S. Sherk, C.-M. Sung, D. Sutton, P.J. Tummino, R.J. Wegrzyn, K.R. Auger, D. Dhanak, ACS Med. Chem. Lett. 1 (2010) 39–43.
19. K. Liu, W. Rao, H. Parikh, Q. Li, T.L Guo, S. Grant, G.E. Kellogg, S. Zhang, Eur. J. Med. Chem. 47 (2012) 125–136.
20. K.-Y., Jung, R. Samadani, J. Chauhan, K. Nevels, J.L. Yap, J. Zhang, S. Worlikar, M.E. Lanning, L. Chen, M. Ensey, S. Shukla, R. Salmo, G. Heinzl, C. Gordon, T. Dukes, A.D. MacKerell, P. Shapiro, Jr, S. Fletcher, Org. Biomol. Chem.11 (2013) 3706–3732.
21. R.D. Taylor, M. MacCoss, A.D.G. Lawson, J. Med. Chem. 57 (2014) 5845–5859.
22. E. Vitaku, D.T. Smith, J.T. Njardarson, J. Med. Chem. 57 (2014) 10257−10274.
23. A. Bolognese, G. Correale, M. Manfra, A. Lavecchia, E., Novellino, V. Barone, Org. Biomol. Chem. 2 (2004) 2809–2813.
24. (a) S. Nekkanti, K. Veeramani, N.P. Kumar, N. Shankaraiah, Green Chem. 18 (2016) 3439–3447; (b) N. Shankaraiah, N. Markandeya, M.-E. Moraga, A. Kamal, L. S. Santos, Synthesis (2009) 2163–2170; (c) S. Nekkanti, K. Veeramani, S.S. Kumari, R. Tokala, N. Shankaraiah, RSC Adv. 6 (2016) 103556–103566.
25. B. Meunier, Acc. Chem. Res. 41 (2008) 69–77.

26. Shaveta, S. Mishra, P. Singh, Eur. J. Med. Chem.124 (2016) 500–536.
27. P. Sharma, K.R. Senwar, M.K. Jeengar, T.S. Reddy, V.G.M. Naidu, A. Kamal, N. Shankaraiah, Eur. J. Med. Chem. 104 (2015) 11–24.
28. K.R. Senwar, T.S. Reddy, D. Thummuri, P. Sharma, S.K. Bharghava, V.G.M. Naidu, N. Shankaraiah, Bioorg. Med. Chem. Lett. 26 (2016) 4061–4069.
29. K.R. Senwar, P. Sharma, T.S. Reddy, M.K. Jeengar, V.L. Nayak, V.G.M. Naidu, A. Kamal, N. Shankaraiah, Eur. J. Med. Chem. 102 (2015) 413–424.
30. C.-C. Liang, A.Y. Park, J.-L. Guan, Nat. Protoc. 2 (2007) 329–333.
31. M.P. Sheetz, D. Felsenfeld, C.G. Galbraith, D. Choquet, Biochem. Soc. Symp. 65 (1999) 233–243.
32. G. Lorente, E. Syriani, M. Morales, PLoS One 9 (2014) e85817.
33. E. Wulf, A. Debobent, F.A. Bautz, H. Faulsticht, T. Wielandt, Proc. Natl. Acad. Sci. USA 76 (1979) 4498–4502.
34. M.L. Circu, T.Y. Aw, Free Radic. Biol. Med. 48 (2010) 749–762.
35. H.U. Simon, A. Haj-Yehia, F. Levi-Schaffer, Apoptosis 5 (2000) 415–418.
36. M. Karbowski, C. Kurono, M. Wozniak, M. Ostrowski, M. Teranishi, Y. Nishizawa, J. Usukura, T. Soji, T. Wakabayashi, Free Radic. Biol. Med. 26 (1999) 396–409.
37. C.P. LeBel, H. Ischiropoulos, S.C. Bondy, Chem. Res. Toxicol. 5 (1992) 227–231.
38. R.A. Gottlieb, FEBS Lett. 482 (2000) 6–12.
39. D. Trachootham, J. Alexandre, P. Huang, Nat. Rev. Drug Discov. 8 (2009) 579–591.
40. T.S. Reddy, H. Kulhari, V.G. Reddy, A.V.S. Rao, V. Bansal, A. Kamal, R. Shukla, Org. Biomol. Chem. 13 (2015) 10136–10149.
41. G. Koopman, C.P. Reutelingsperger, G.A. Kuijten, R.M. Keehnen, S.T. Pals, M.H. van Oers, Blood 84 (1994) 1415–1420.

Table 1. Time and yield data of newly synthesized compounds **17a–t** using conventional and microwave irradiation method.

Compound	Conventional Method[a]		Microwave Method[b]	
	time (h)	% yield[c]	time (min)	% yield[c]
17a	8	61	6	79
17b	7	63	5	85
17c	8	61	5	82
17d	10	71	8	86
17e	5	67	8	79
17f	5	57	8	74
17g	5	64	7	76
17h	5	65	7	78
17i	5	59	7	76
17j	5	61	7	78
17k	9	65	10	85
17l	6	64	7	80
17m	7	66	7	80
17n	8	58	8	78
17o	6	67	8	84
17p	6	62	8	88
17q	11	70	10	91
17r	5	63	5	95
17s	5	79	5	92
17t	5	66	5	88

[a]Conventional Method: Toluene, piperidine (cat.), reflux, 5–11 h.

[b]Microwave-assisted synthesis: Toluene, piperidine (cat.), 150 ^{o}C, 5–10 min.

[c]Isolated yields

Table 2. IC_{50} values (in µM) of benzimidazole-thiazolidinediones **17a–t** on selected human cancer cell lines and a normal kidney cell (HeK-293T)[a]

Compound	MDAMB-231[b]	PC-3[c]	HeLa[d]	A549[e]	HT1080[f]	HeK-293T[g]
17a	6.83	11.97	1.67	3.57	3.12	13.6
17b	13.6	8.72	7.83	0.57	2.43	21.7
17c	24.53	6.32	15.4	1.84	6.35	15.3
17d	7.78	2.98	5.22	5.11	4.45	14.1
17e	14.90	5.94	16.3	2.93	1.68	18.79
17f	>50	>50	7.51	8.93	3.32	>50
17g	21.3	11.7	0.51	0.66	1.12	35.7
17h	34.92	14.66	23.27	0.98	3.65	21.5
17i	>50	>50	6.89	14.5	8.76	>50
17j	2.88	8.37	4.78	0.91	2.47	12.7
17k	NT	NT	NT	NT	NT	NT
17l	2.29	2.50	0.95	0.67	0.66	8.21
17m	3.26	4.37	1.44	0.93	4.58	18.9
17n	1.78	0.63	0.18	0.13	0.19	3.35
17o	0.27	10.24	2.24	0.53	0.98	16.6
17p	29.10	>50	0.32	0.13	0.27	6.76
17q	4.37	0.11	0.25	0.096	0.16	6.65
17r	>50	>50	26.26	0.88	0.57	13.57
17s	NT	NT	NT	NT	NT	NT
17t	2.04	0.43	7.48	0.74	0.59	27.8
N[h]	-	-	2.83	1.87	-	-

[a]50% inhibitory concentration after 48 h of compound treatment; [b]breast cancer cells; [c]prostate cancer cells; [d]cervical cancer cells; [e]lung cancer cells; [f]bone cancer cells; [g]Normal Kidney cells; [h] N: Nocodazole as standard; NT - not tested.

Figure captions

Figure 1. The structure of some bioactive thiazolidinediones and benzimidazoles.

Figure 2. The design of small molecules bearing benzimidazole-thiazolidinedione as anticancer agents.

Figure 3. Effect of compounds **17p** and **17q** on migration potential of A549 cells. Cells were exposed to IC_{50} concentrations of **17p** and **17q** and scratched with sterile 200 µL pipette tip. The images were captured at 0, 24 and 48 h using phase contrast microscope.

Figure 4. Effects of compounds **17p** and **17q** on F-actin polymerisation in A549 cancer cells. The cells were treated with IC_{50} concentrations of **17p** and **17q** and stained with

Rhodamine-phalloidin (red fluorescent dye: actin filament) and Hoechst 33242 (nucleus: blue).

Figure 5. Effect of compounds **17p** and **17q** on nuclear morphology of A549. Cells were treated with IC_{50} concentrations of **17p** and **17q** and stained with Hoechst 33242 for 24 h. Images were captured by a fluorescence microscope (Nikon).

Figure 6. Effect of compounds **17p** and **17q** on intracellular reactive oxygen species (ROS) production. A549 Cells were treated with IC_{50} concentrations of **17p** and **17q** for 24 h and stained with DCFH-DA and photographed using fluorescence microscope (Nikon).

Figure 7. Compound **17p** and **17q** triggered change in mitochondrial membrane potential (DΨm). (a) A549 cells were treated with Control-DMSO and IC_{50} concentrations **17p** and **17q** and processed by rhodamine-123 staining followed by flow cytometry analysis. The peak change to the left indicate depolarization. (b) Data shown are mean ± SD from three independent experiments.

Figure 8. Annexin V- FITC/propidium iodide dual staining assay. A549 cells were treated with IC_{50} concentrations of **17p** and **17q** and stained with Annexin V-FITC/PI and analysed for apoptosis using flow cytometer. The 10,000 cells from each sample were analysed by flow cytometry. The percentage of cells positive for Annexin V-FITC and/or Propidium iodide is reported inside the quadrants. Cells in the lower left quadrant (Q2-LL: AV-/PI-): live cells; lower right quadrant (Q2-LR: AV+/PI-): early apoptotic cells; upper right quadrant (Q2-UR: AV+/PI+): late apoptotic cells and upper left quadrant (Q2-UL: AV-/PI+): necrotic cells.

Scheme captions

Scheme 1. Synthesis of thiazolidinedione **2** and *N*-substituted thiazolidinediones **6a**–**d**, **8a**–**c** and **10**.

Scheme 2. Synthesis of benzimidazole-thiazolidinedione derivatives **17a**–**t**.

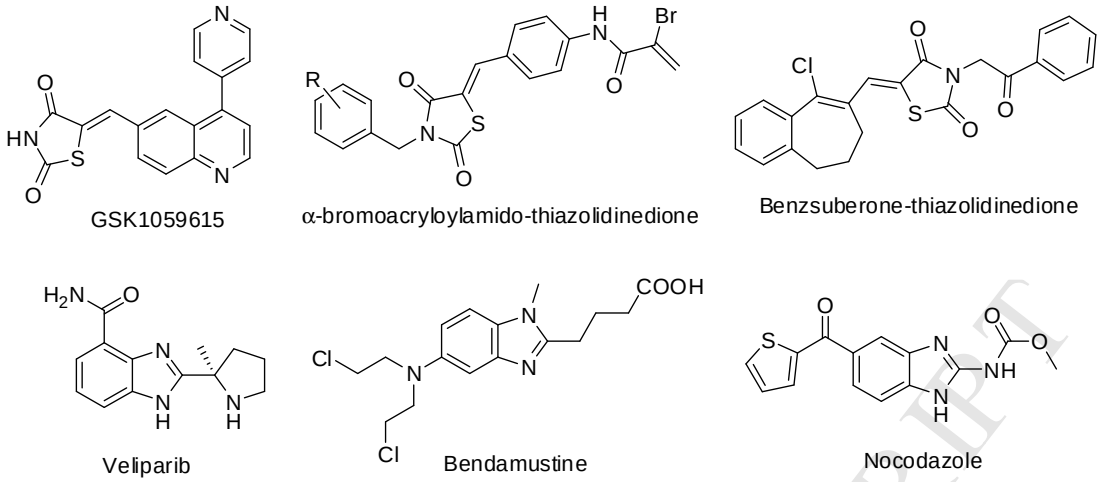

Figure 1. The structure of some bioactive thiazolidinediones and benzimidazoles.

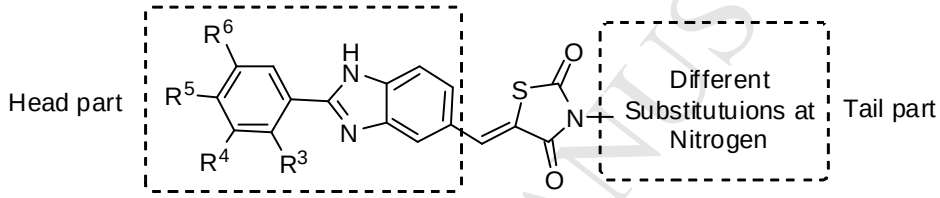

Figure 2. The design of small molecules bearing benzimidazole-thiazolidinedione as anticancer agents.

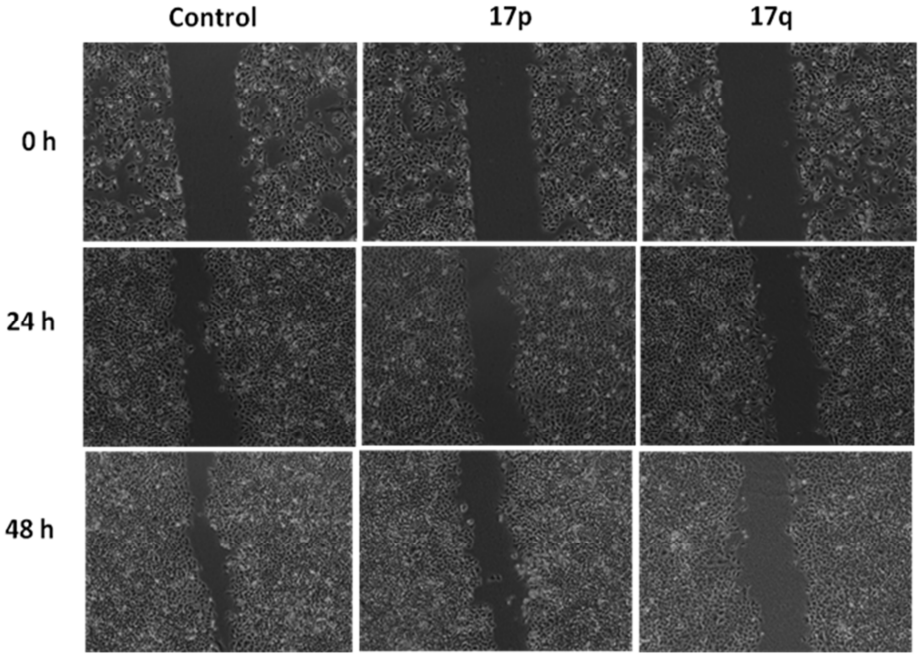

Figure 3. Effect of compounds **17p** and **17q** on migration potential of A549 cells. Cells were exposed to IC_{50} concentrations of **17p** and **17q** and scratched with sterile 200 µL pipette tip. The images were captured at 0, 24 and 48 h using phase contrast microscope.

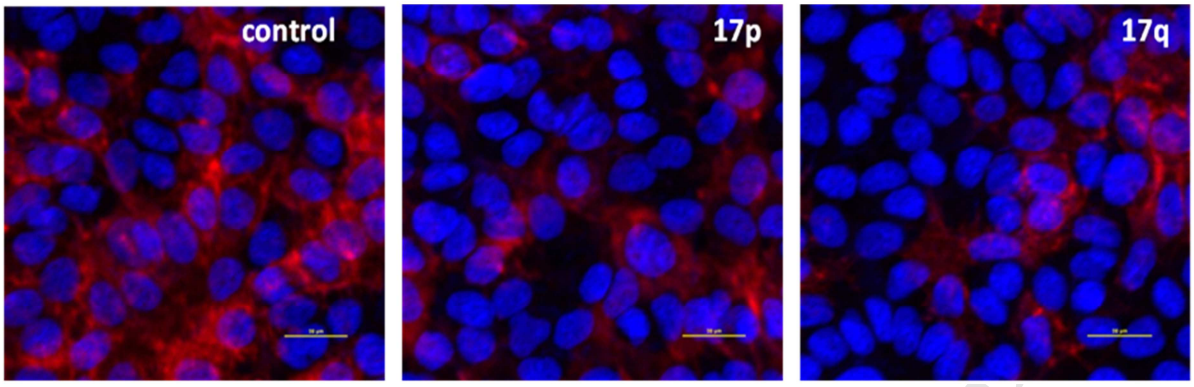

Figure 4. Effects of compounds **17p** and **17q** on F-actin polymerisation in A549 cancer cells. The cells were treated with IC_{50} concentrations of **17p** and **17q** and stained with Rhodamine-phalloidin (red fluorescent dye: actin filament) and Hoechst 33242 (nucleus: blue).

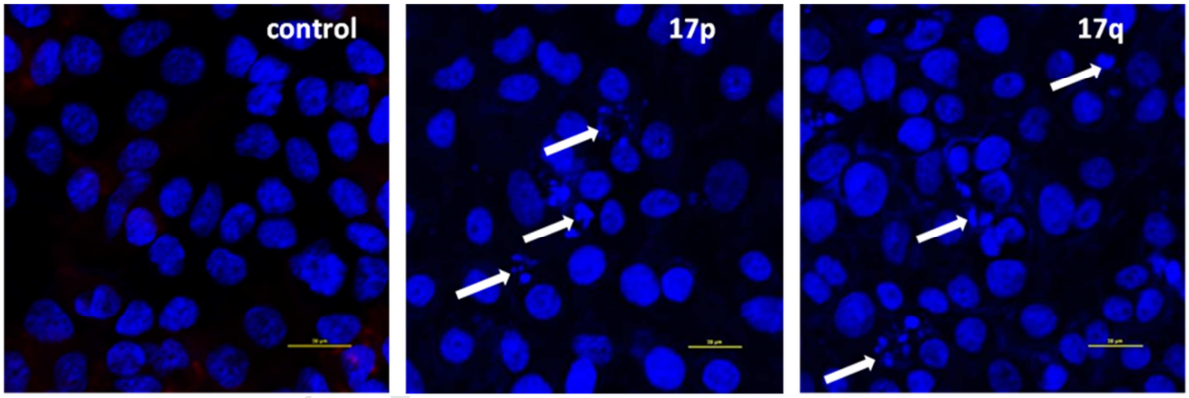

Figure 5. Effect of compounds **17p** and **17q** on nuclear morphology of A549. Cells were treated with IC_{50} concentrations of **17p** and **17q** and stained with Hoechst 33242 for 24 h. Images were captured by a fluorescence microscope (Nikon).

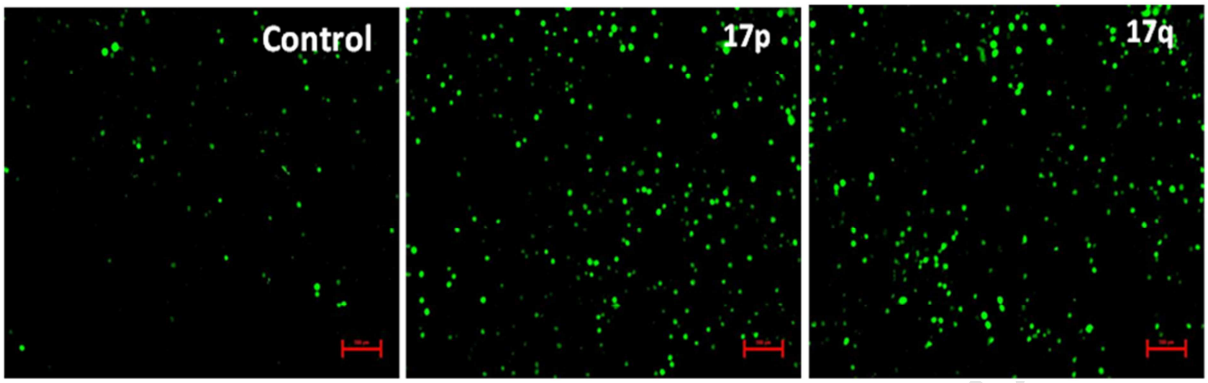

Figure 6. Effect of compounds **17p** and **17q** on intracellular reactive oxygen species (ROS) production. A549 Cells were treated with IC_{50} concentrations of **17p** and **17q** for 24 h and stained with DCFH-DA and photographed using fluorescence microscope (Nikon).

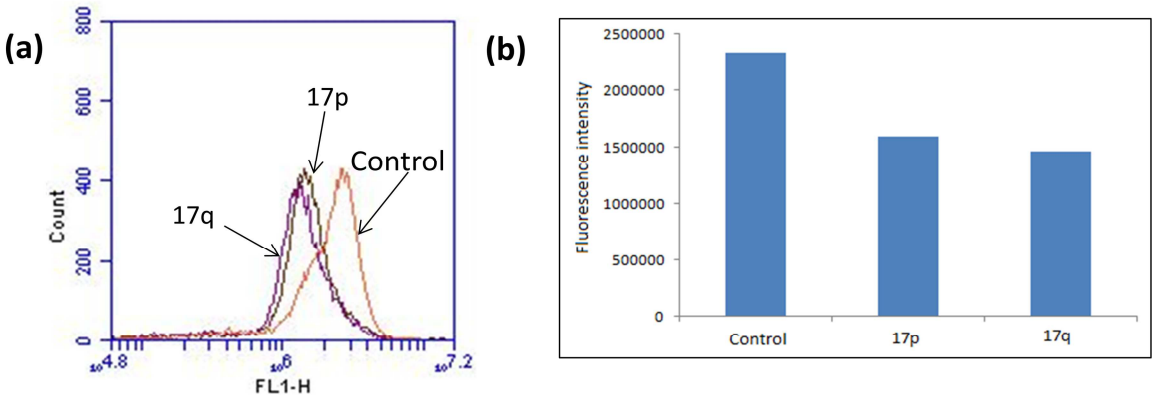

Figure 7. Compound **17p** and **17q** triggered change in mitochondrial membrane potential (DΨm). (a) A549 cells were treated with Control-DMSO and IC_{50} concentrations **17p** and **17q** and processed by rhodamine-123 staining followed by flow cytometry analysis. The peak change to the left indicate depolarization. (b) Data shown are mean ± SD from three independent experiments.

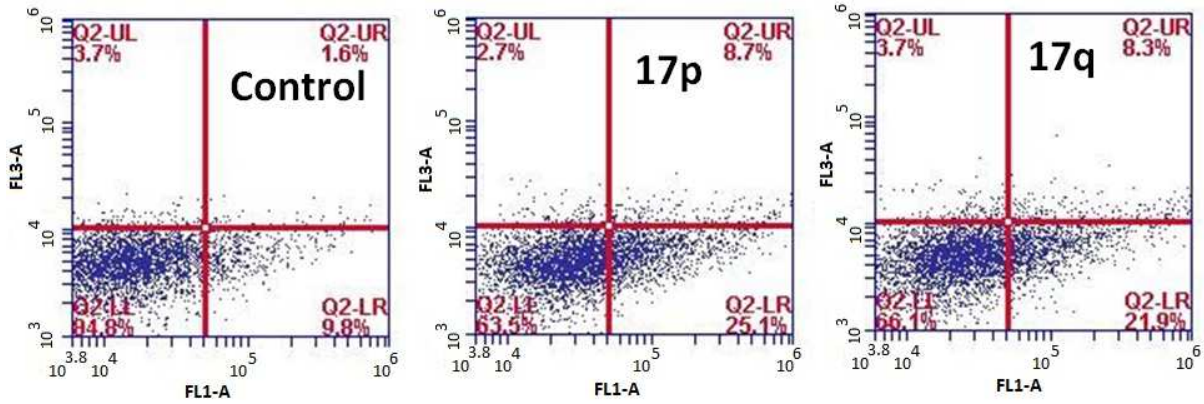

Figure 8. Annexin V- FITC/propidium iodide dual staining assay. A549 cells were treated with IC_{50} concentrations of **17p** and **17q** and stained with Annexin V-FITC/PI and analysed for apoptosis using flow cytometer. The 10,000 cells from each sample were analysed by flow cytometry. The percentage of cells positive for Annexin V-FITC and/or Propidium iodide is reported inside the quadrants. Cells in the lower left quadrant (Q2-LL: AV-/PI-): live cells; lower right quadrant (Q2-LR: AV+/PI-): early apoptotic cells; upper right quadrant (Q2-UR: AV+/PI+): late apoptotic cells and upper left quadrant (Q2-UL: AV-/PI+): necrotic cells.

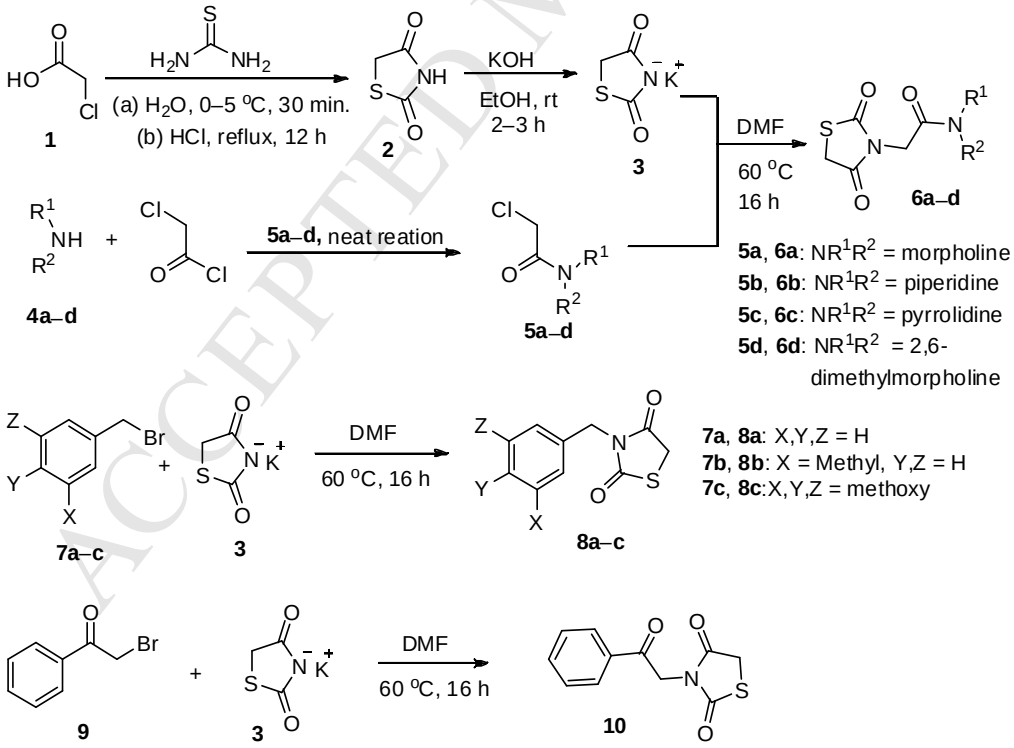

Scheme 1. Synthesis of thiazolidinedione **2** and *N*-substituted thiazolidinediones **6a**–**d**, **8a**–**c** and **10**.

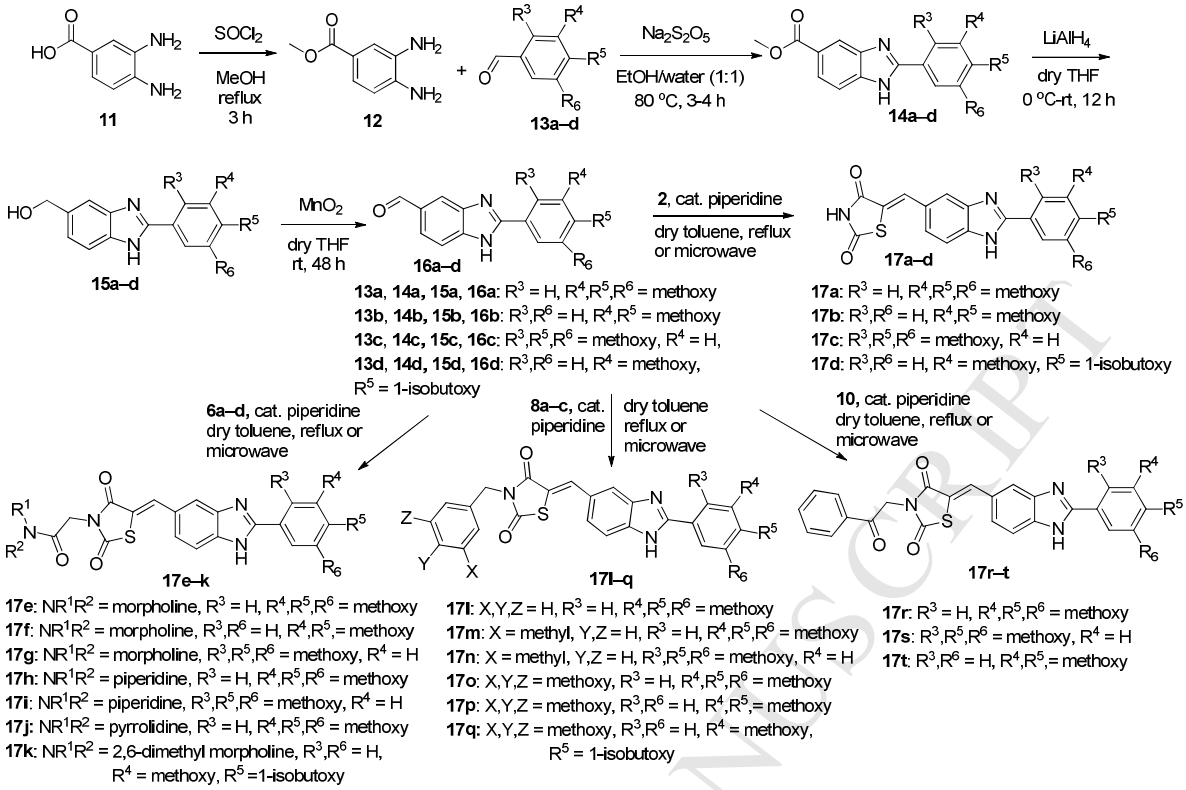

Scheme 2. Synthesis of benzimidazole-thiazolidinedione derivatives **17a**–**t**.

Research Highlights

- Conventional and microwave-assisted synthesis of 1*H*-benzimidazole-thiazolidinediones
- Cytotoxicity on selected human cancer cell lines and a normal cell line
- Induction of apoptosis by test compounds **17p** and **17q**
- **17p** and **17q** inhibited cell migration and caused disruption of F-actin protein
- **17p** and **17q** caused the collapse of DΨm and increased the level of ROS

Supporting information

Conventional and microwave-assisted synthesis of new 1*H*-benzimidazole-thiazolidinedione derivatives: A potential anticancer scaffold

Pankaj Sharma,[a] T. Srinivasa Reddy,[b] Niggula Praveen Kumar,[a] Kishna Ram Senwar,[a] Suresh K. Bhargava,[b]* Nagula Shankaraiah[a]*

[a]*Department of Medicinal Chemistry, National Institute of Pharmaceutical Education and Research (NIPER), Hyderabad 500 037, India*
[b]*Centre for Advanced Materials & Industrial Chemistry (CAMIC), School of Science, RMIT University, GPO BOX 2476, Melbourne-3001, Australia*

*Corresponding author

Dr. Nagula Shankaraiah: shankar@niperhyd.ac.in; shankarnbs@gmail.com

Dr. Suresh K. Bhargava: suresh.bhargava@rmit.edu.au

1.0. Copies of ^{1}H NMR and ^{13}C NMR spectra

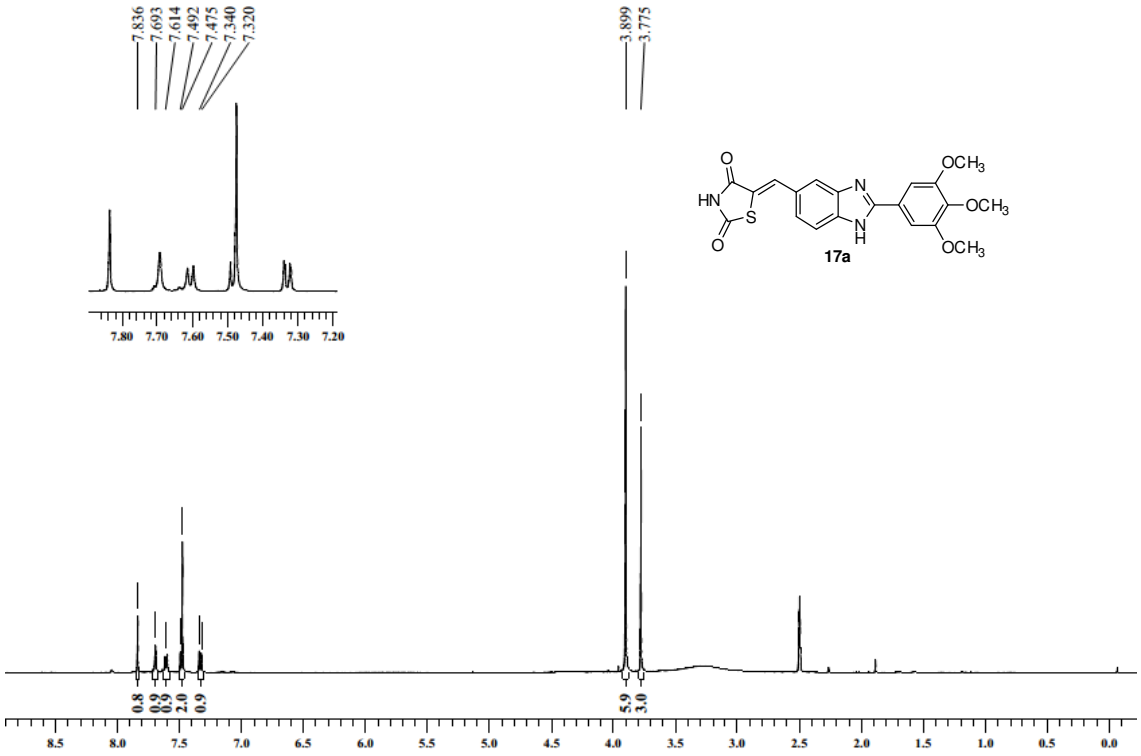

^{1}H NMR (500 MHz, $CDCl_3$+DMSO-d_6) spectrum of compound **17a**

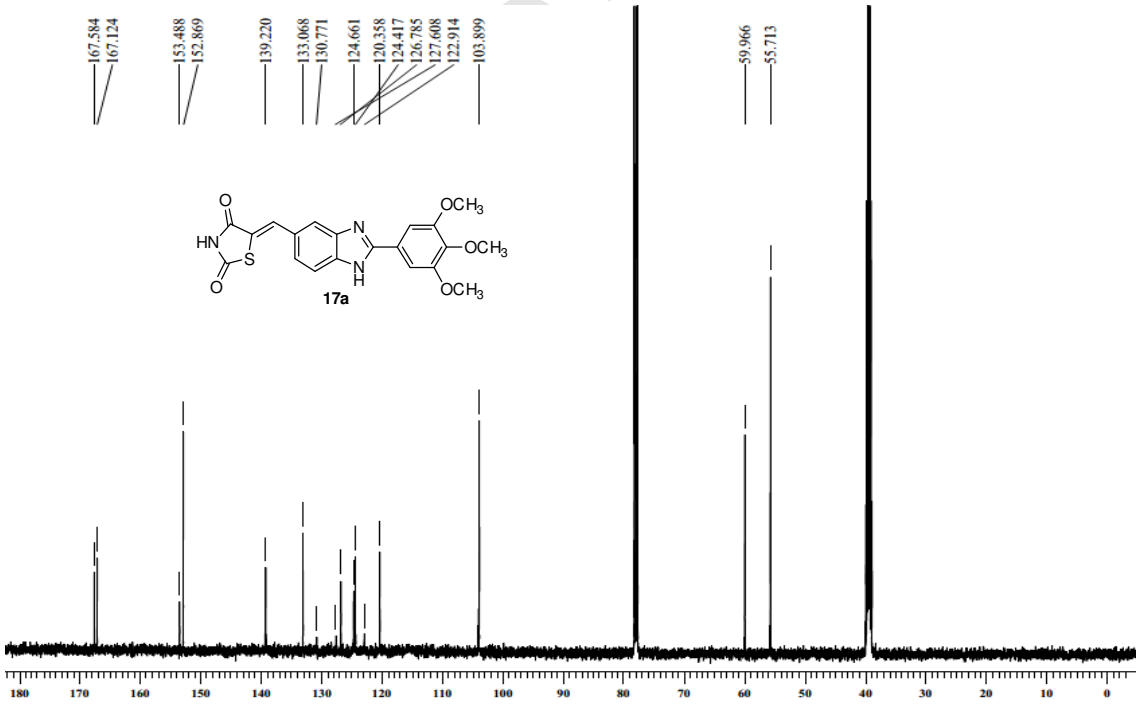

^{13}C NMR (125 MHz, $CDCl_3$+DMSO-d_6) spectrum of compound **17a**

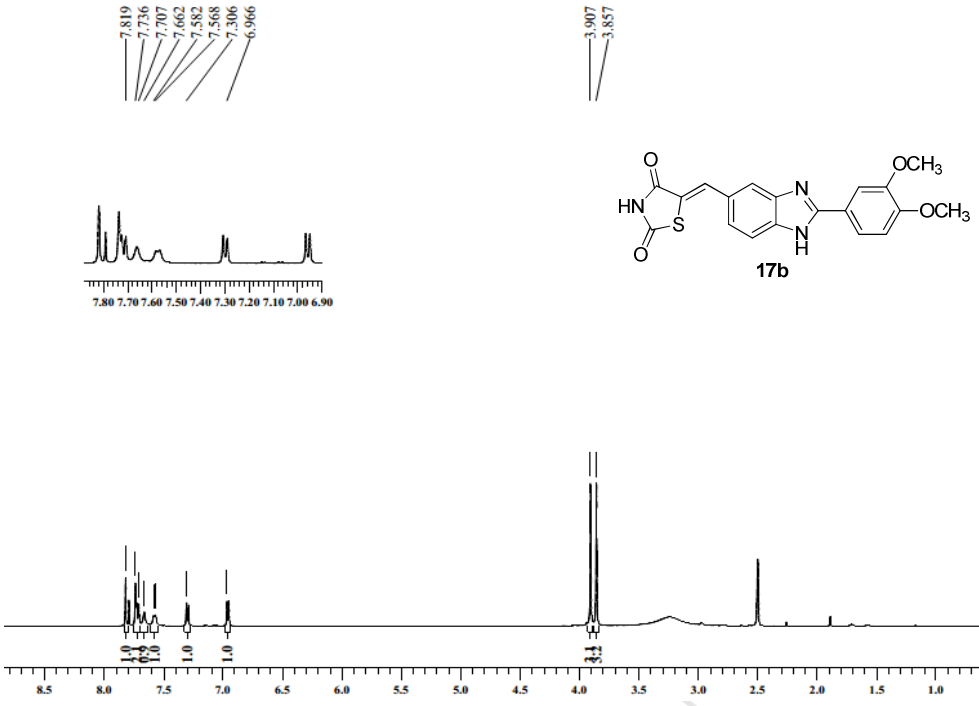

^{1}H NMR (500 MHz, $CDCl_3$+DMSO-d_6) spectrum of compound **17b**

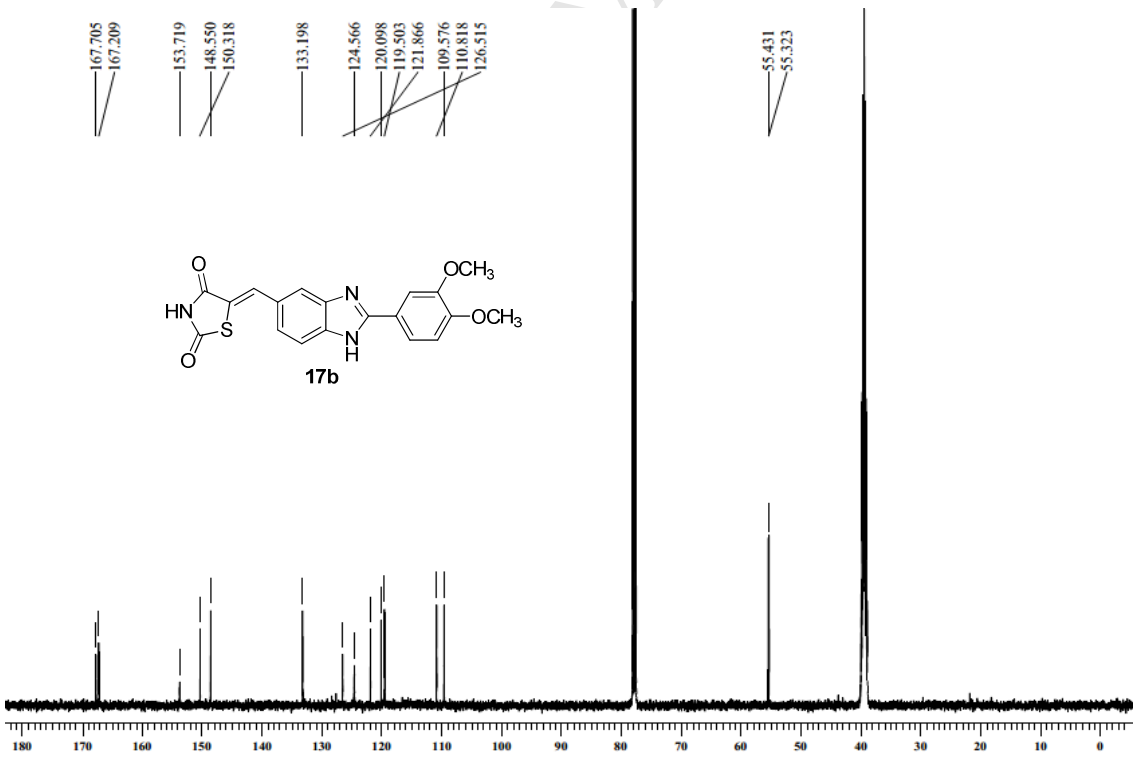

^{13}C NMR (125 MHz, $CDCl_3$+DMSO-d_6) spectrum of compound **17b**

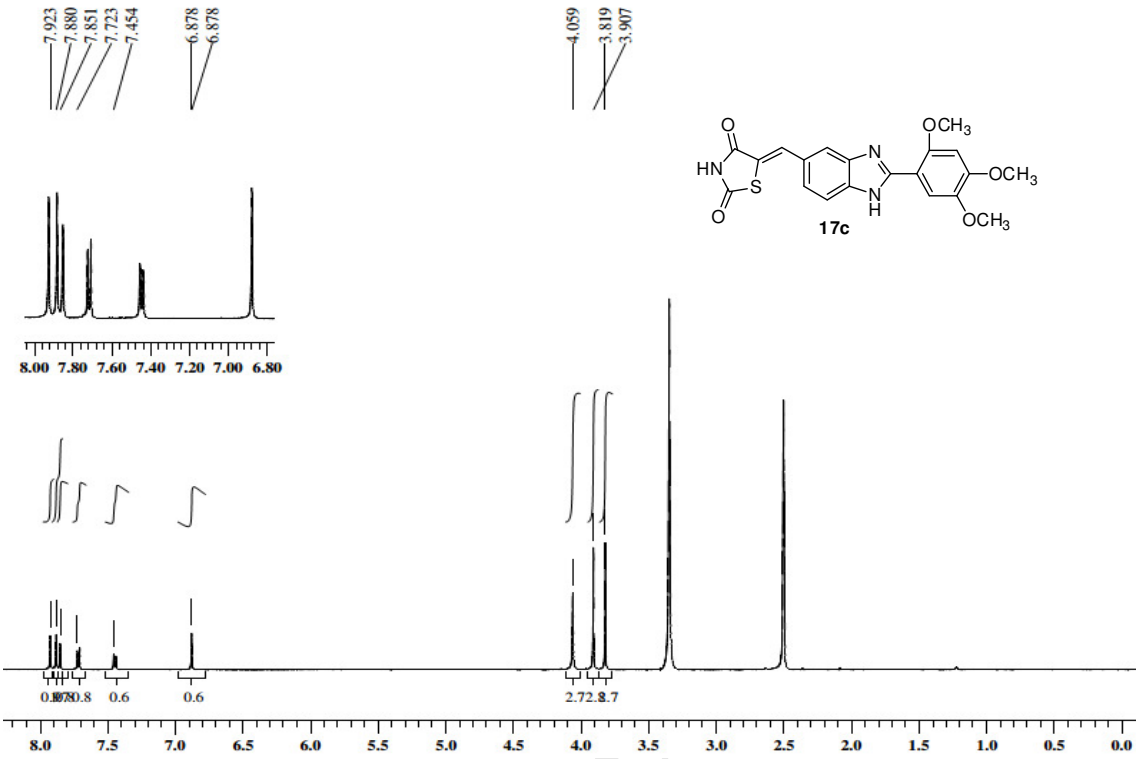

^{1}H NMR (500 MHz, DMSO-d_6) spectrum of compound **17c**

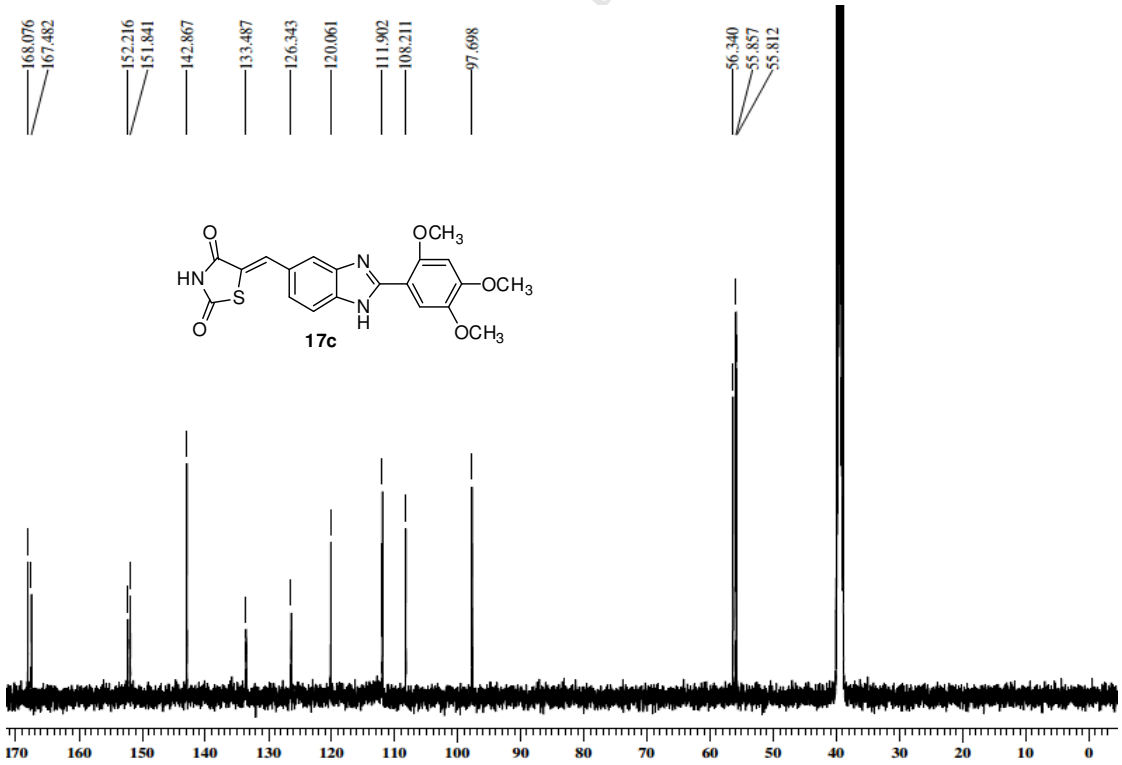

^{13}C NMR (125 MHz, DMSO-d_6) spectrum of compound **17c**

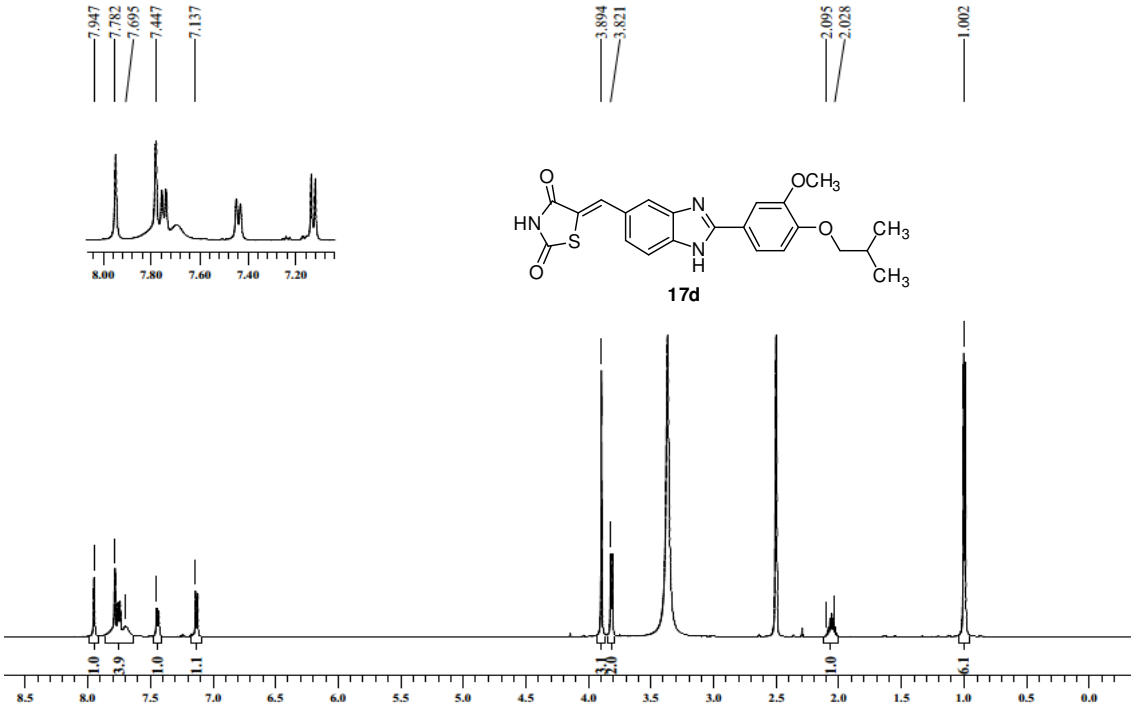

^{1}H NMR (500 MHz, DMSO-d_6) spectrum of compound **17d**

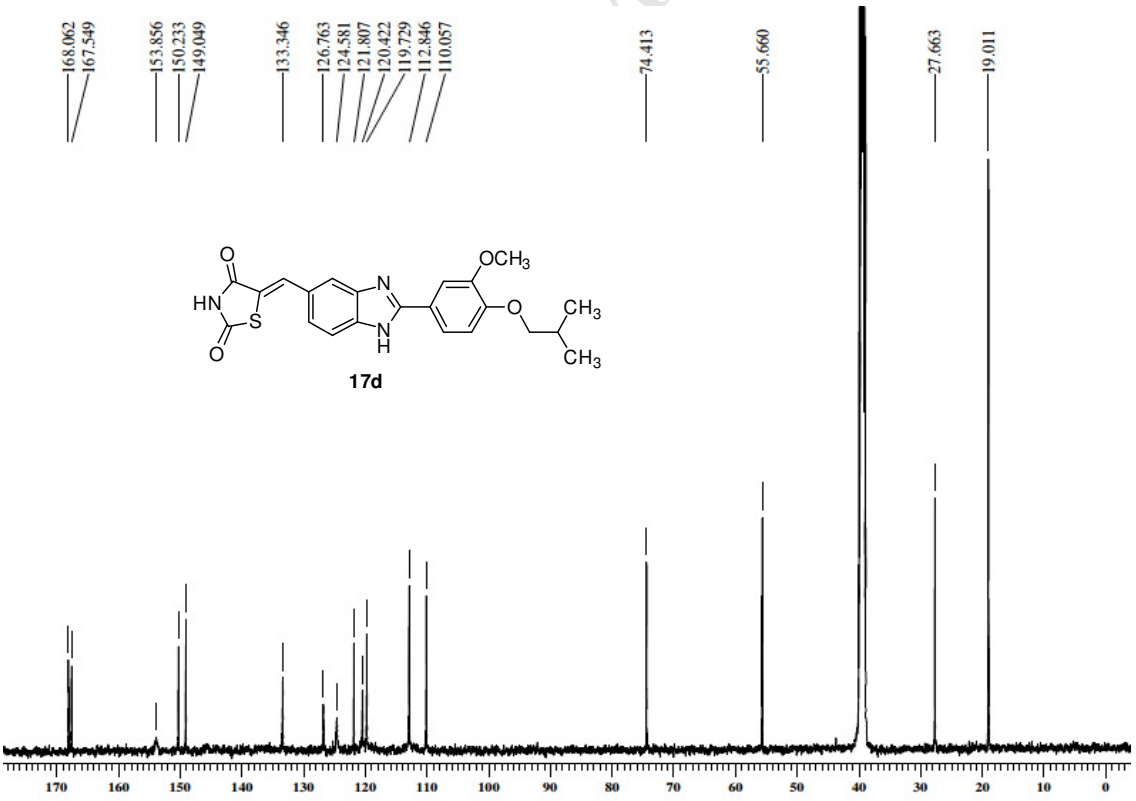

^{13}C NMR (125 MHz, DMSO-d_6) spectrum of compound **17d**

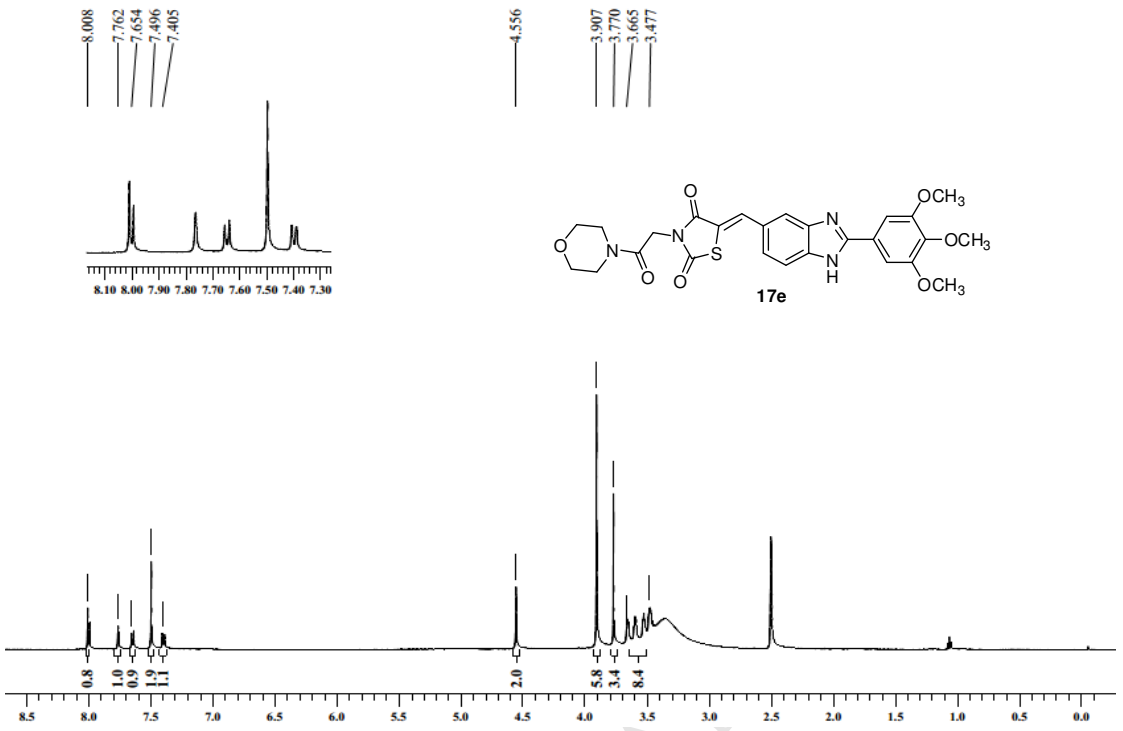

^{1}H NMR (500 MHz, $CDCl_3$+DMSO-d_6) spectrum of compound **17e**

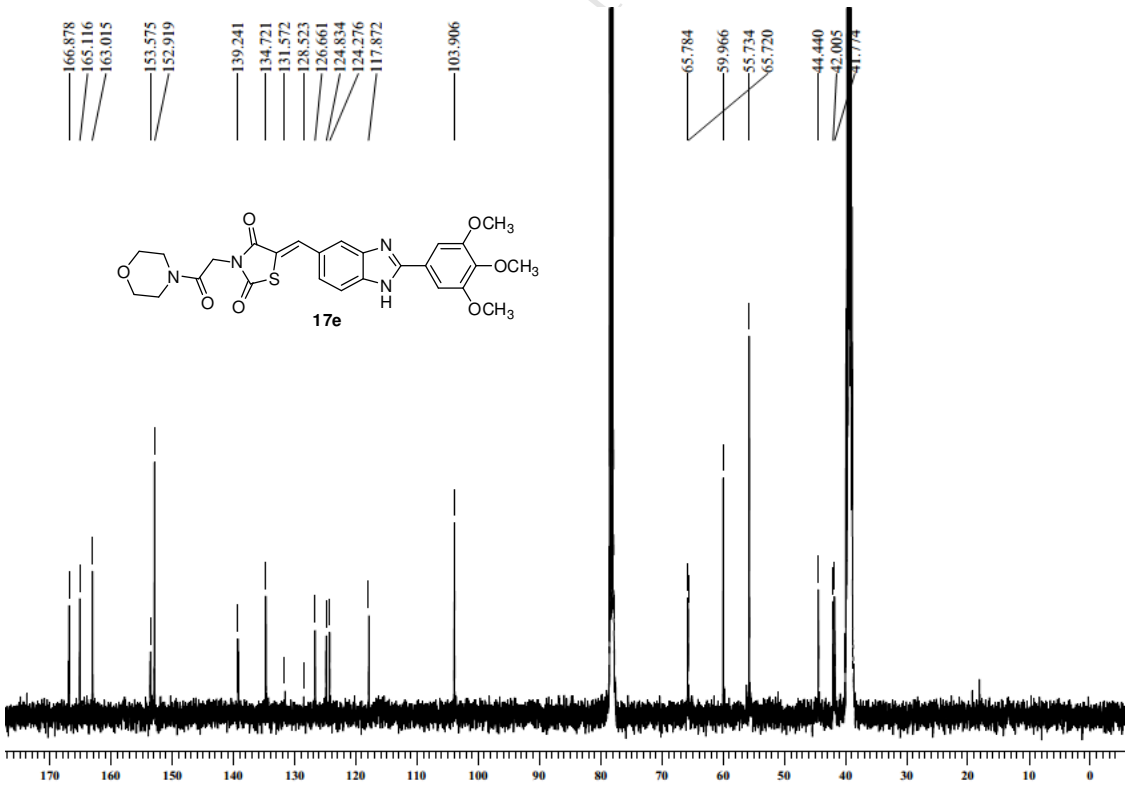

^{13}C NMR (125 MHz, $CDCl_3$+DMSO-d_6) spectrum of compound **17e**

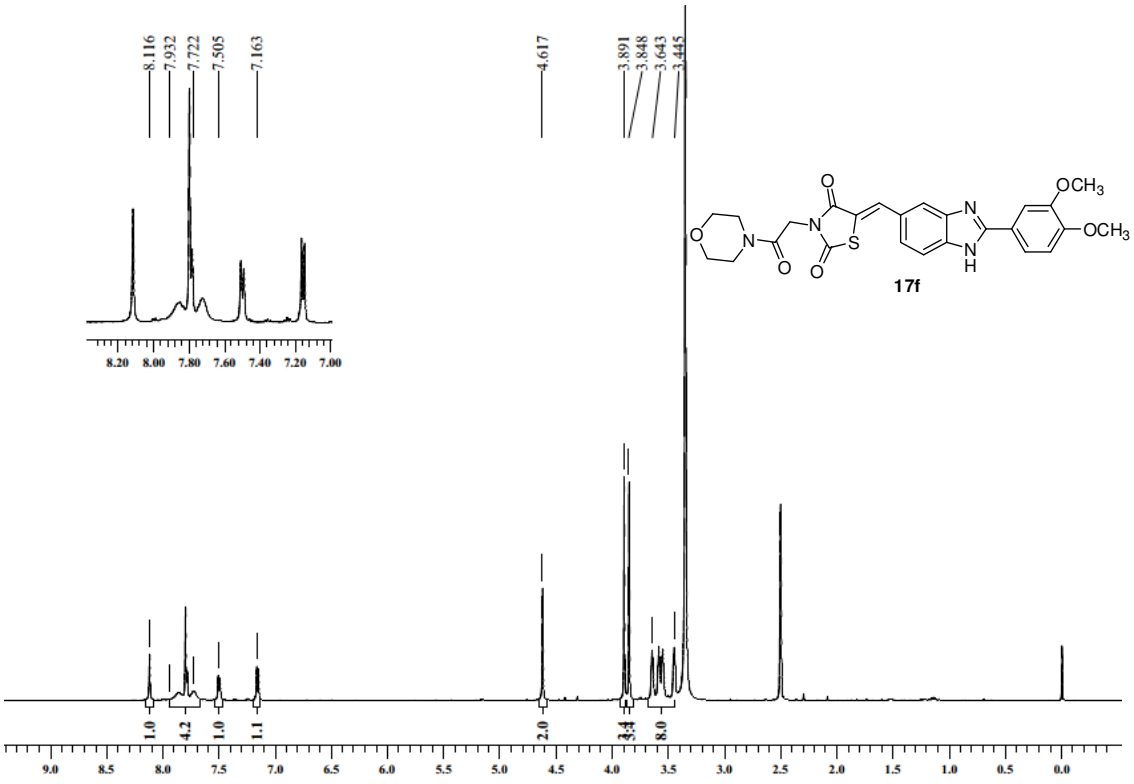

^{1}H NMR (500 MHz, $CDCl_3$+DMSO-d_6) spectrum of compound **17f**

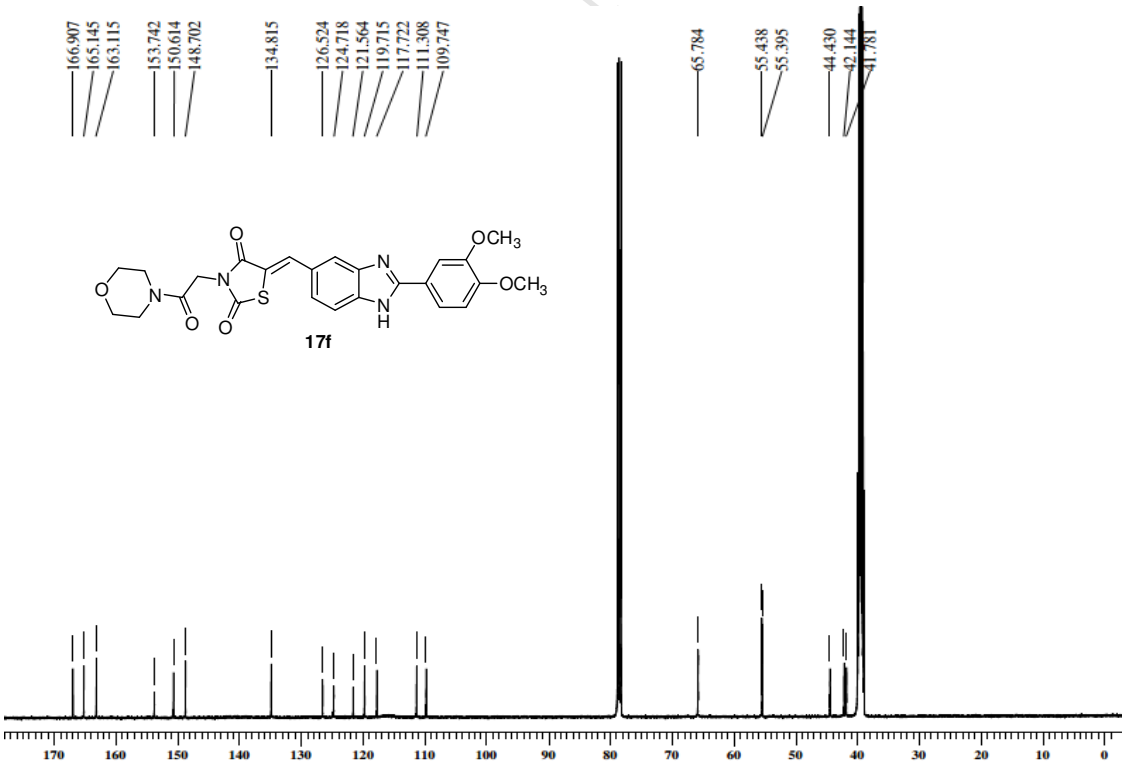

^{13}C NMR (125 MHz, $CDCl_3$+DMSO-d_6) spectrum of compound **17f**

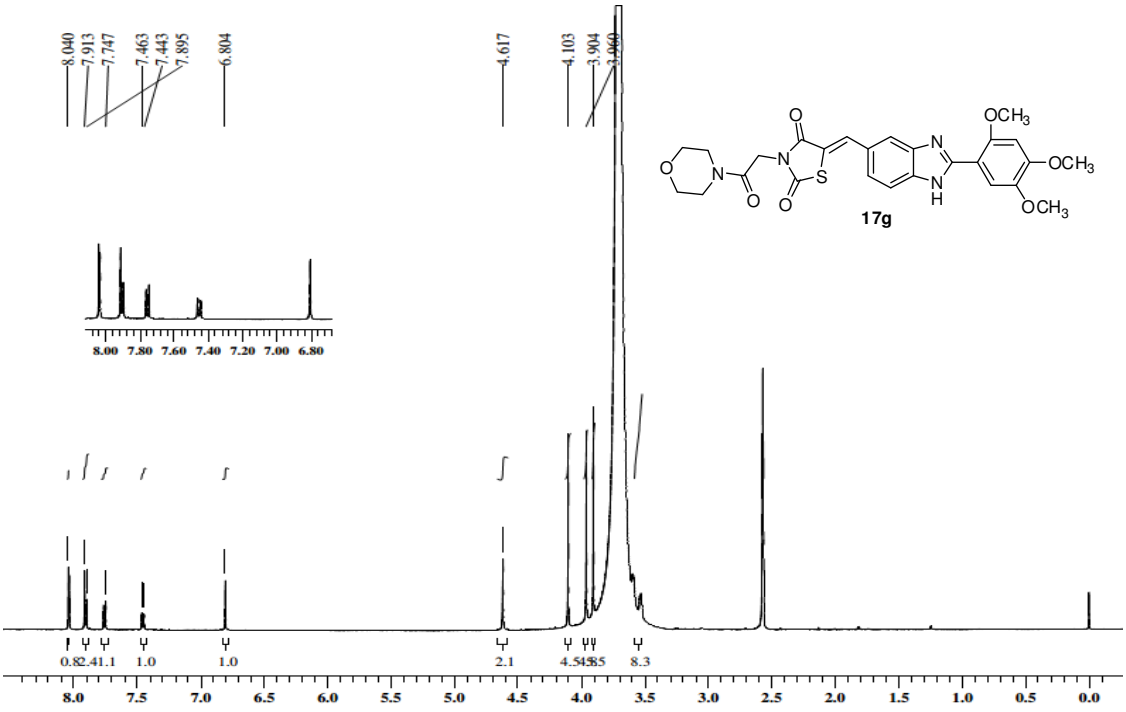

^{1}H NMR (500 MHz, $CDCl_3$+DMSO-d_6) spectrum of compound **17g**

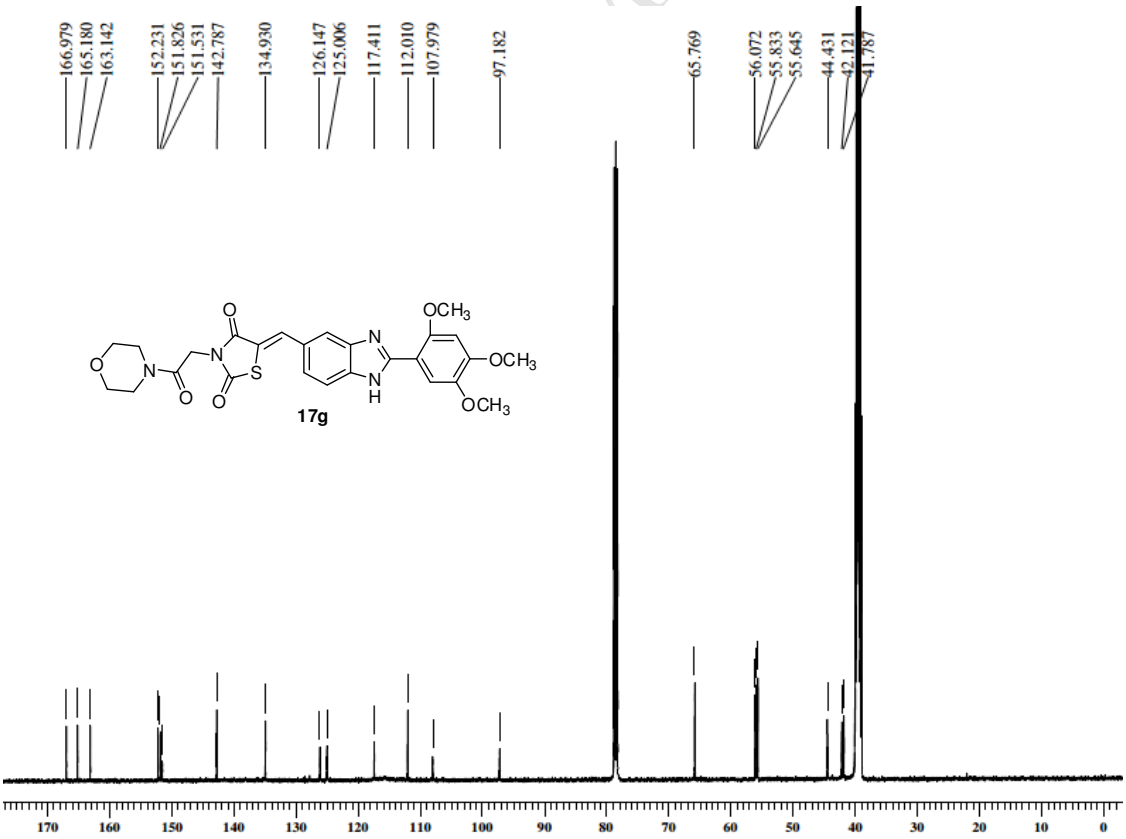

^{13}C NMR (125 MHz, $CDCl_3$+DMSO-d_6) spectrum of compound **17g**

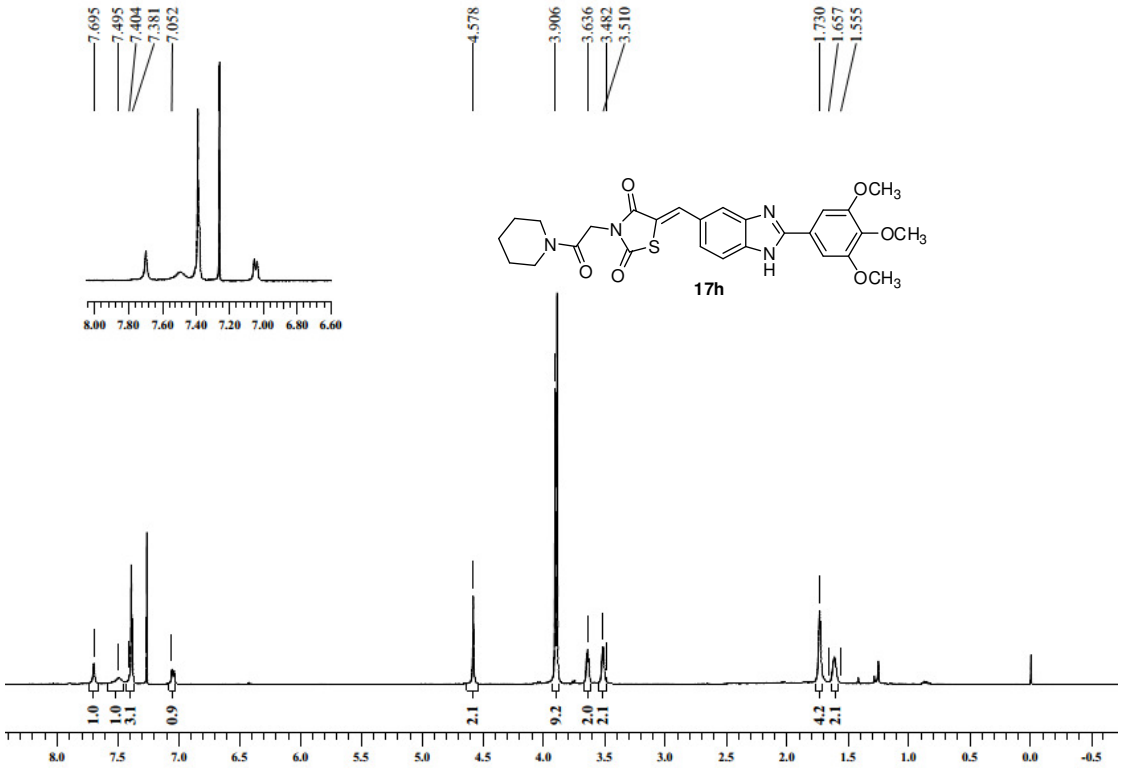

^{1}H NMR (500 MHz, $CDCl_3$+DMSO-d_6) spectrum of compound **17h**

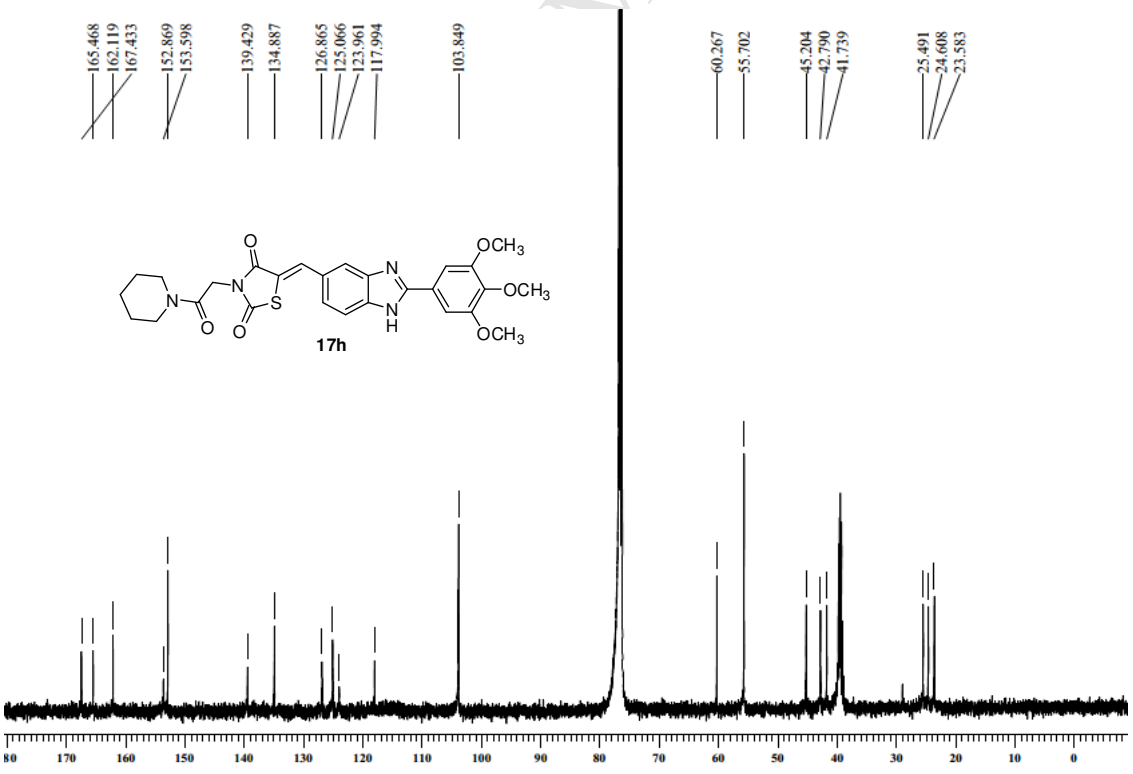

^{13}C NMR (125 MHz, $CDCl_3$+DMSO-d_6) spectrum of compound **17h**

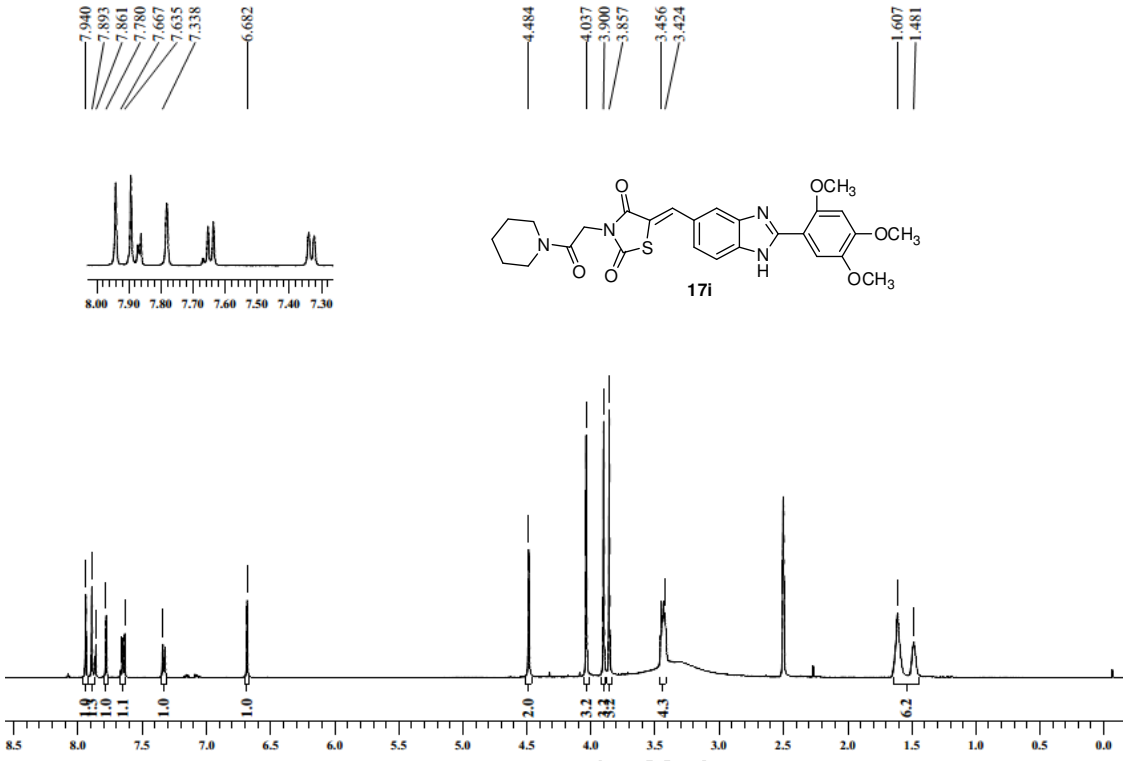

^{1}H NMR (500 MHz, $CDCl_3$+DMSO-d_6) spectrum of compound **17i**

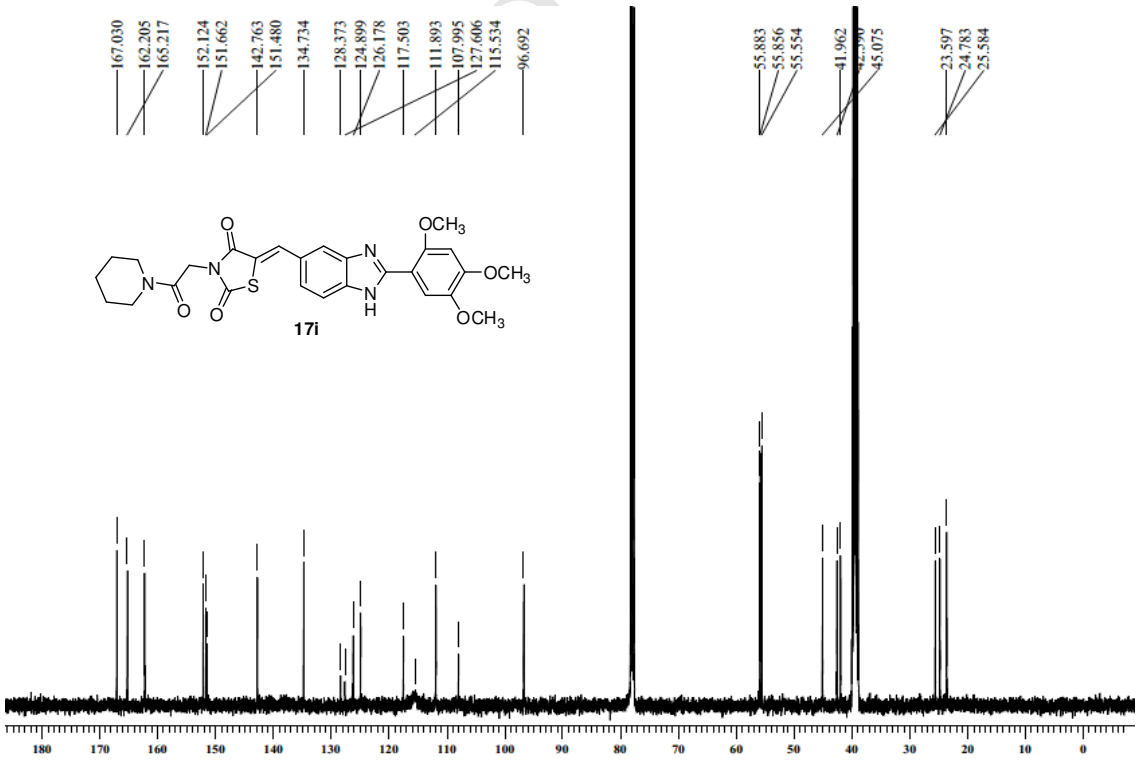

^{13}C NMR (125 MHz, $CDCl_3$+DMSO-d_6) spectrum of compound **17i**

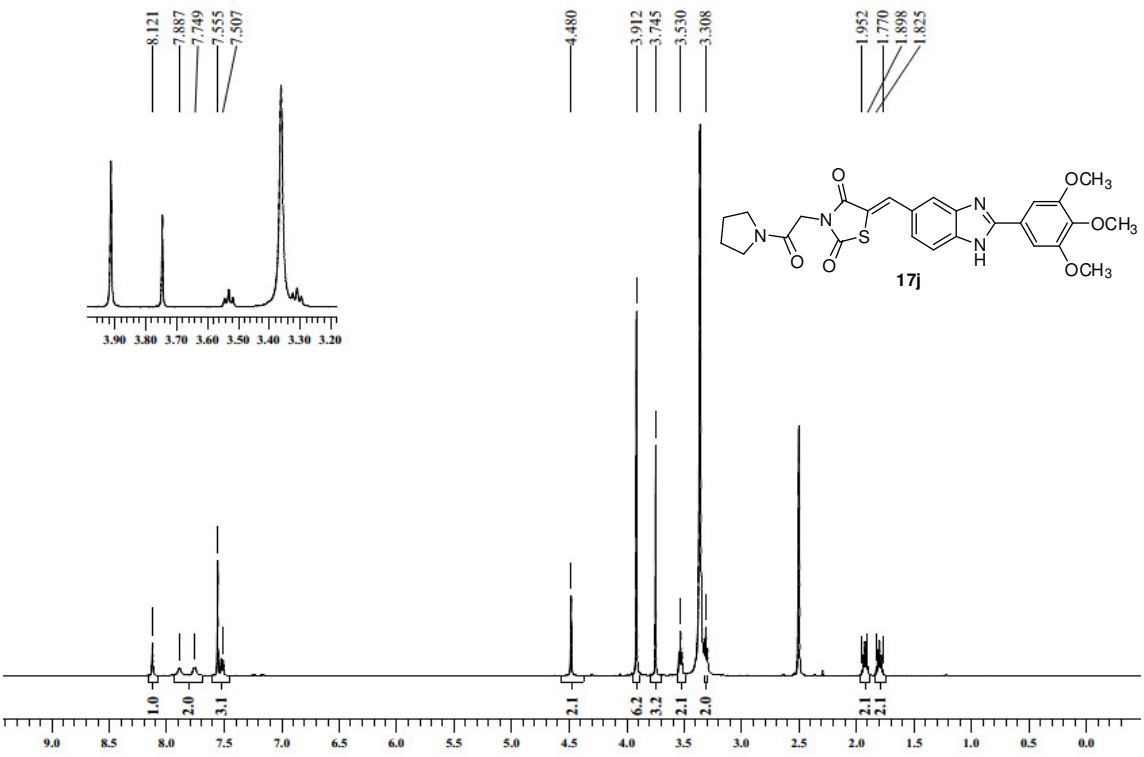

^{1}H NMR (500 MHz, $CDCl_3$+DMSO-d_6) spectrum of compound **17j**

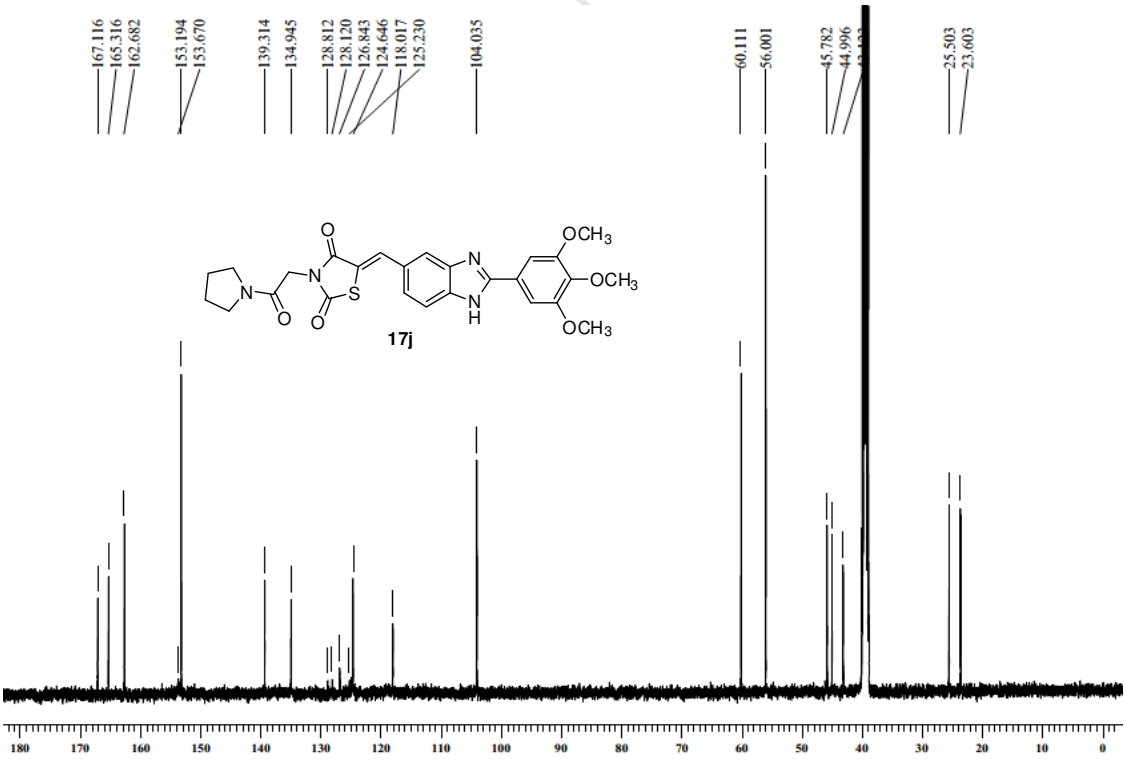

^{13}C NMR (125 MHz, DMSO-d_6) spectrum of compound **17j**

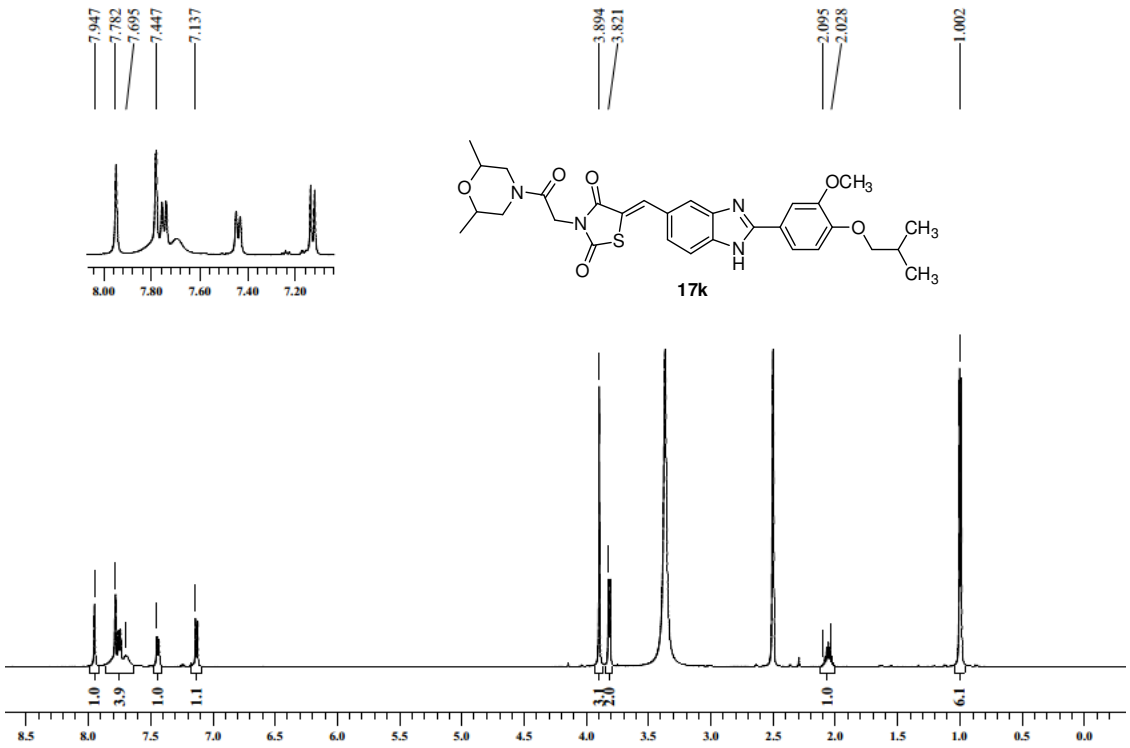

^{1}H NMR (500 MHz, $CDCl_3$+DMSO-d_6) spectrum of compound **17k**

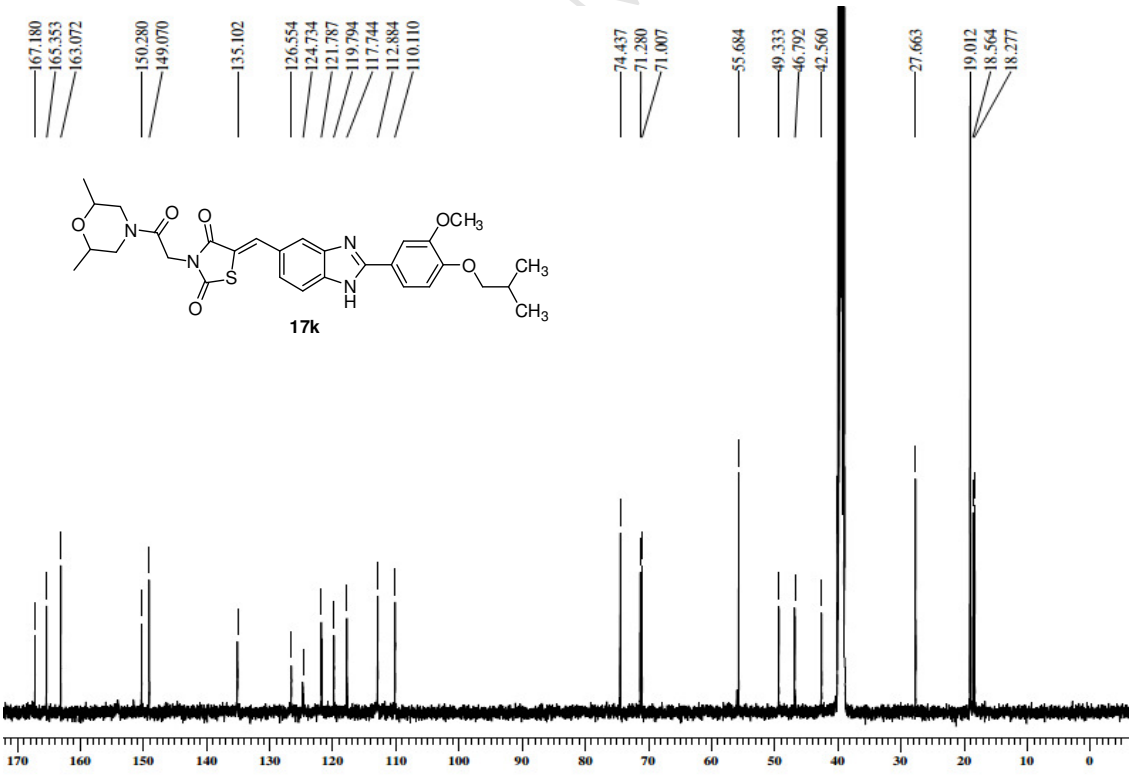

^{13}C NMR (125 MHz, $CDCl_3$+DMSO-d_6) spectrum of compound **17k**

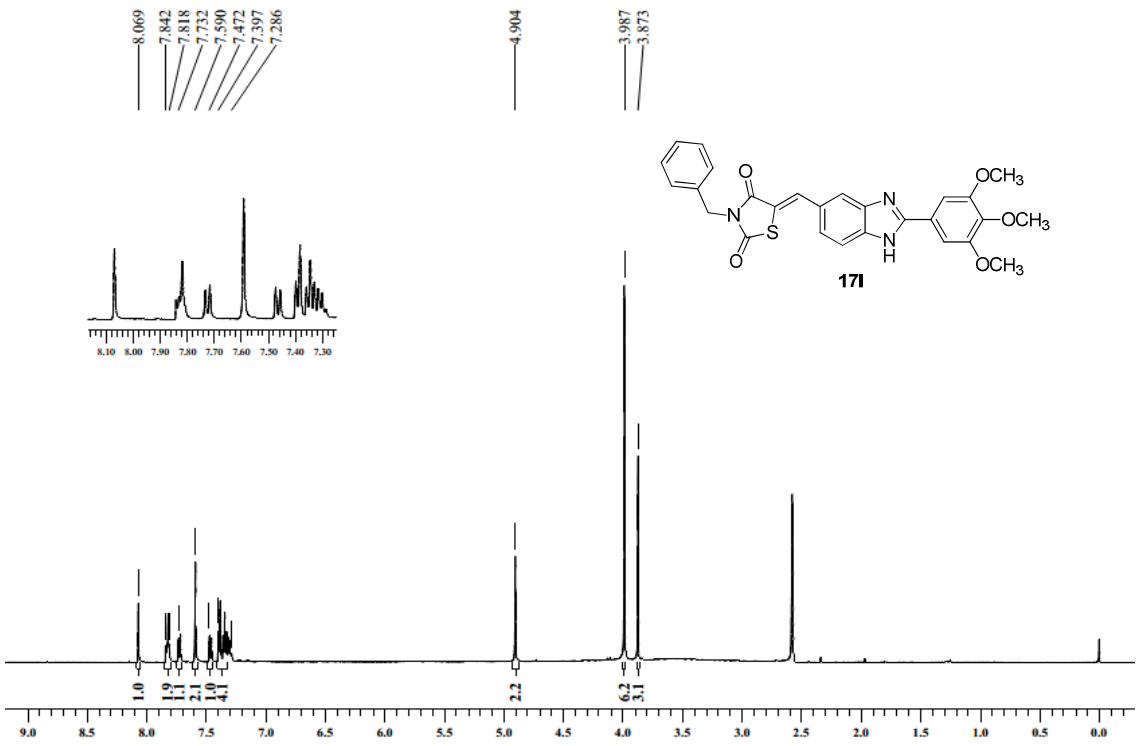

^{1}H NMR (500 MHz, $CDCl_3$+DMSO-d_6) spectrum of compound **17l**

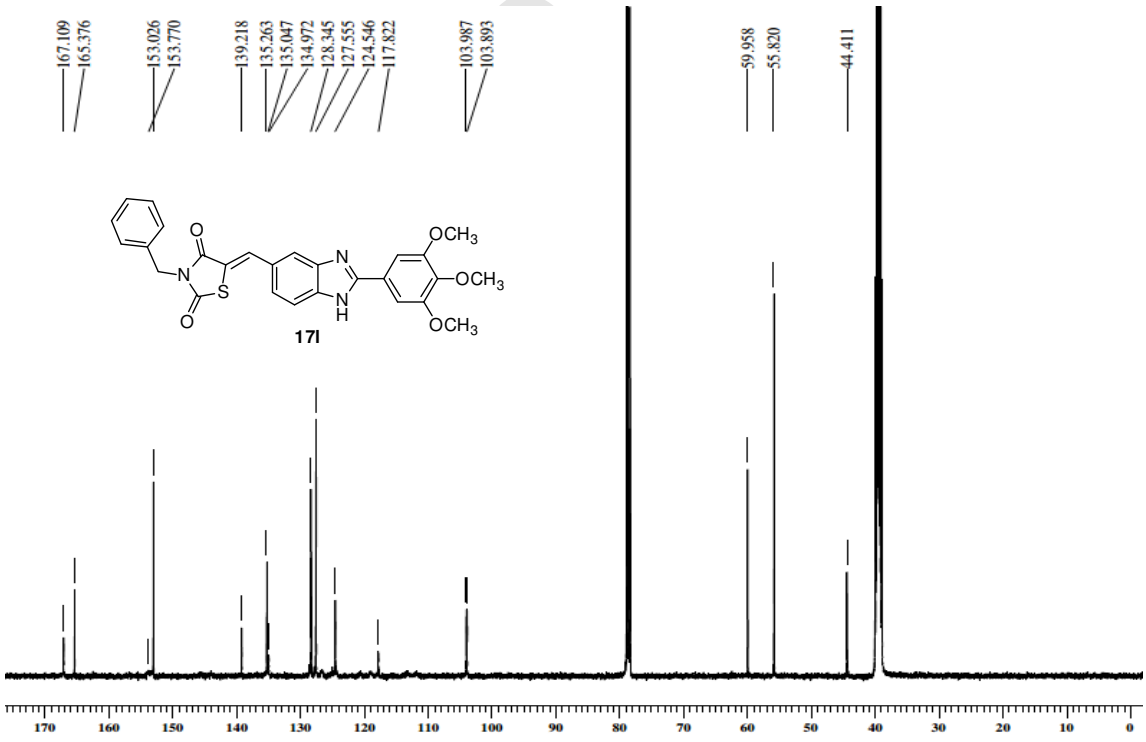

^{13}C NMR (125 MHz, $CDCl_3$+DMSO-d_6) spectrum of compound **17l**

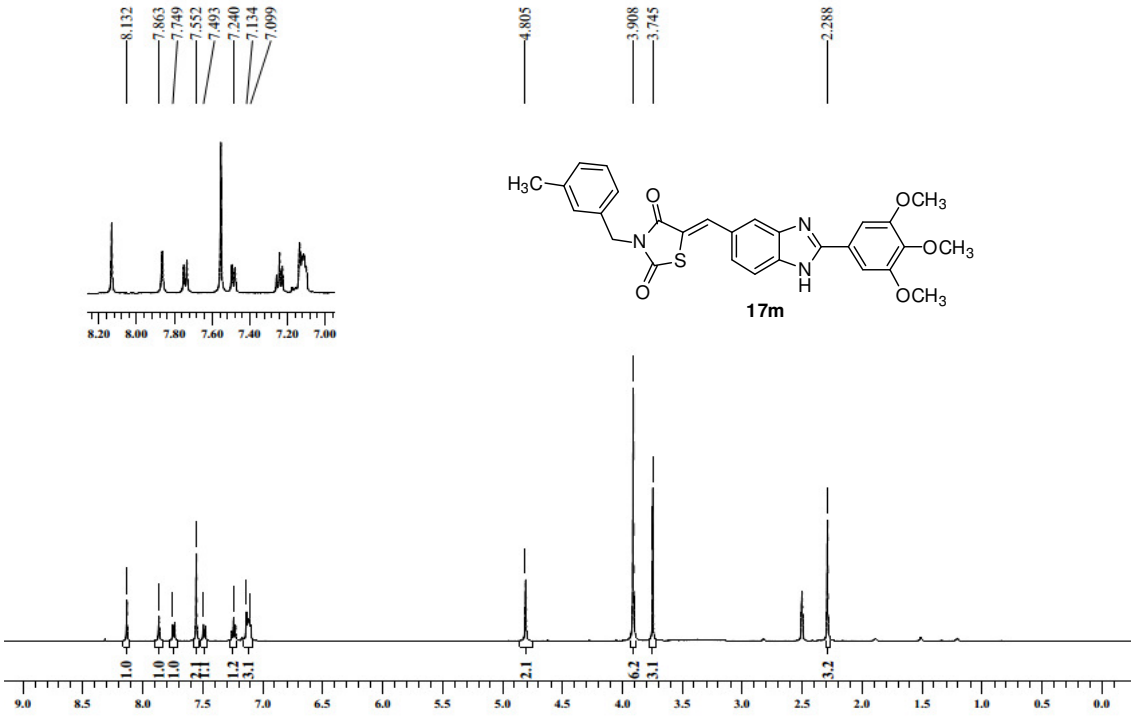

^{1}H NMR (500 MHz, $CDCl_3$+DMSO-d_6) spectrum of compound **17m**

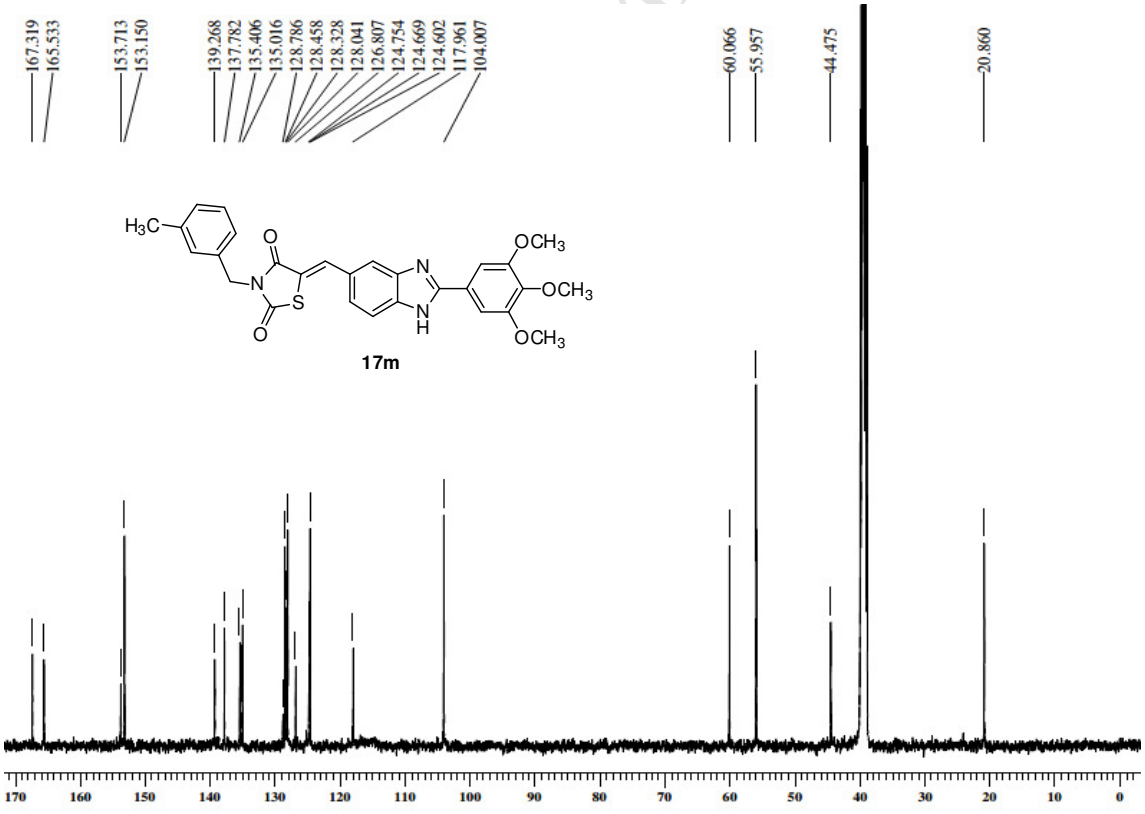

^{13}C NMR (125 MHz, DMSO-d_6) spectrum of compound **17m**

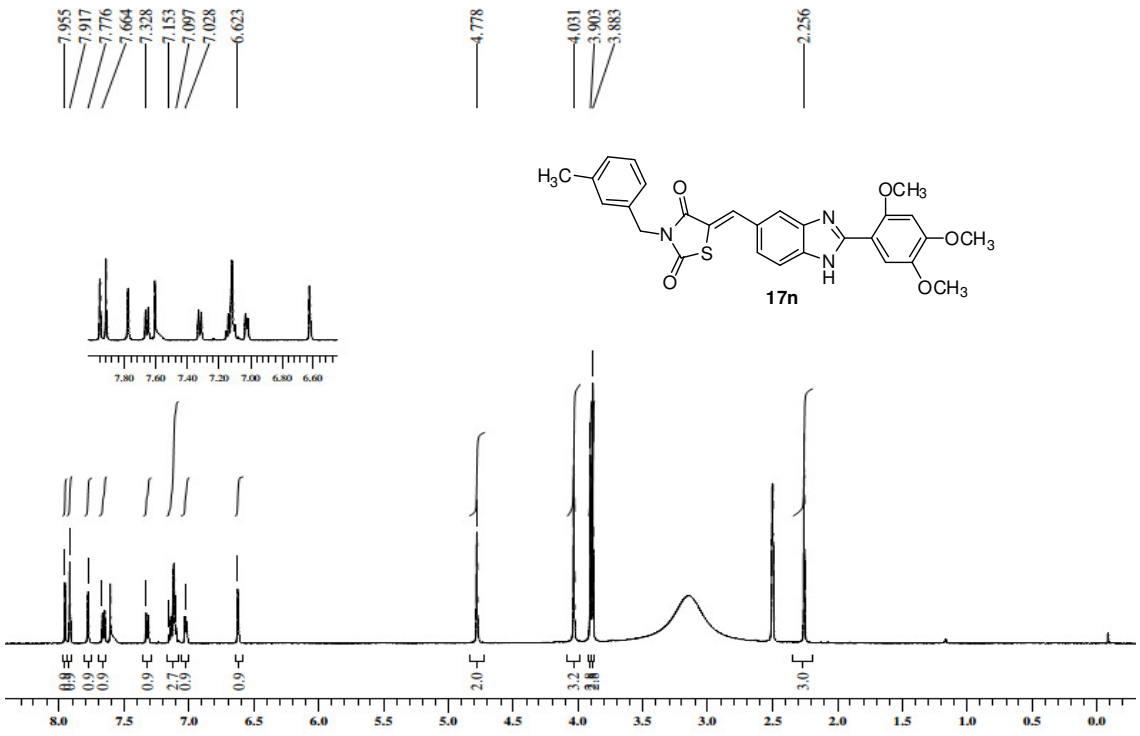

^{1}H NMR (500 MHz, $CDCl_3$+DMSO-d_6) spectrum of compound **17n**

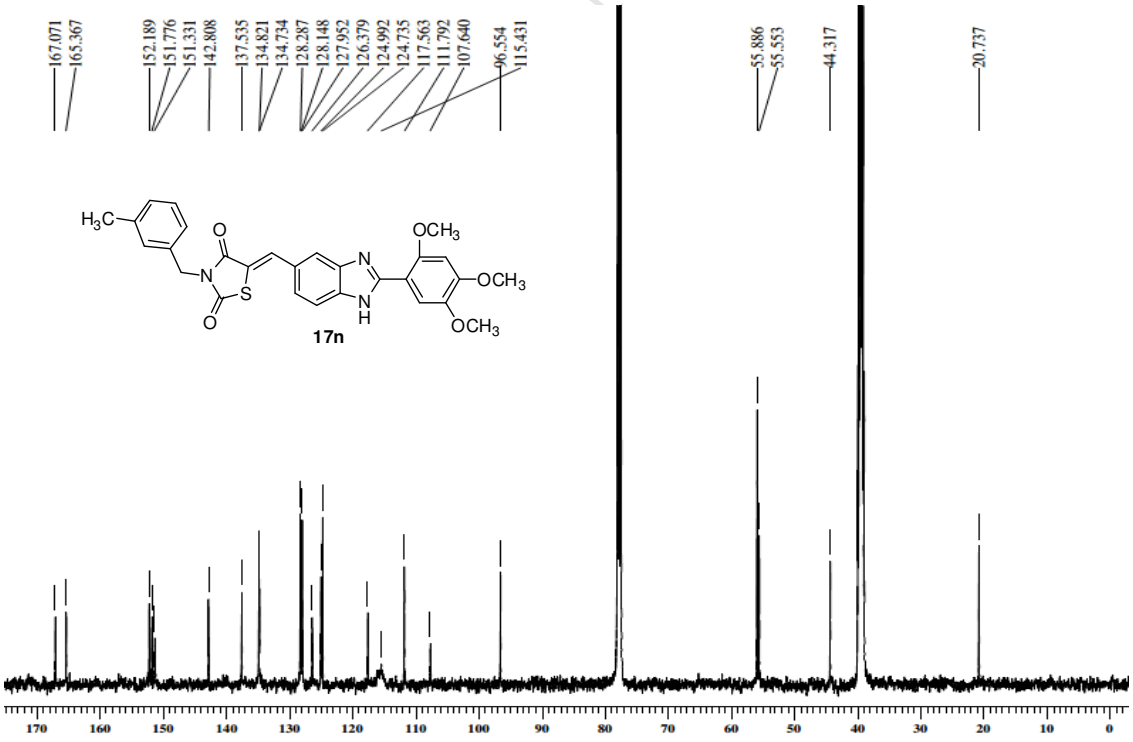

^{13}C NMR (125 MHz, $CDCl_3$+DMSO-d_6) spectrum of compound **17n**

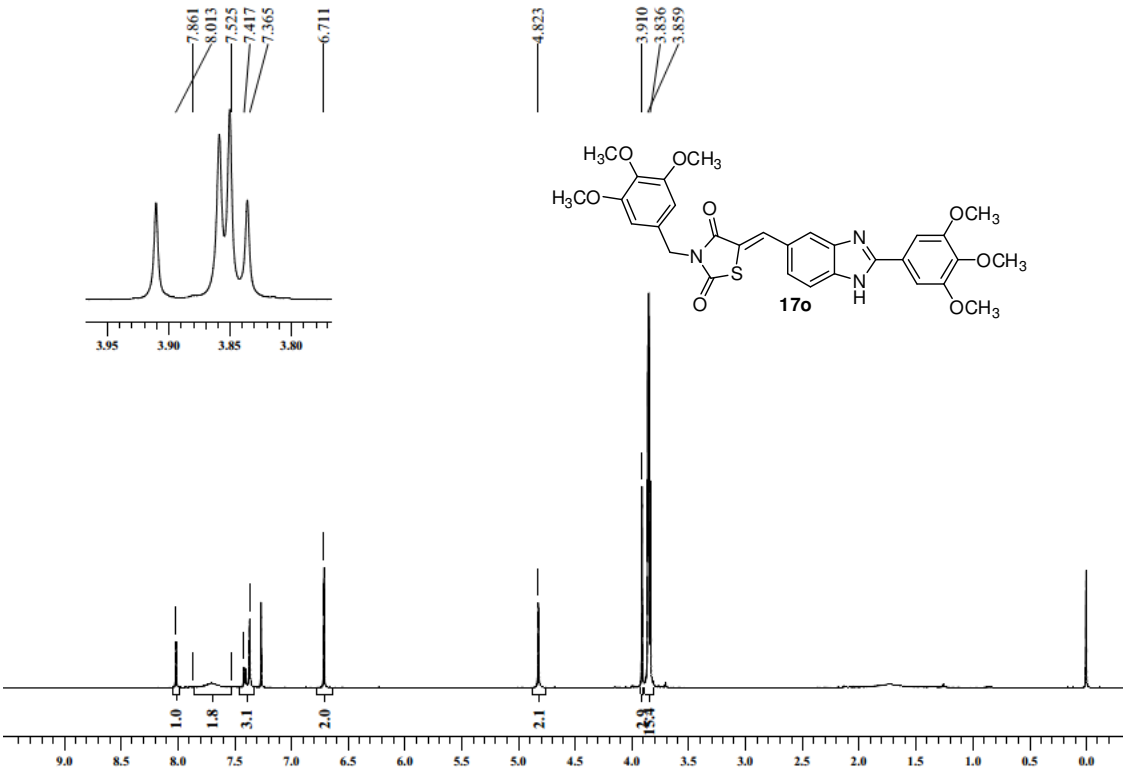

^{1}H NMR (500 MHz, $CDCl_3$) spectrum of compound **17o**

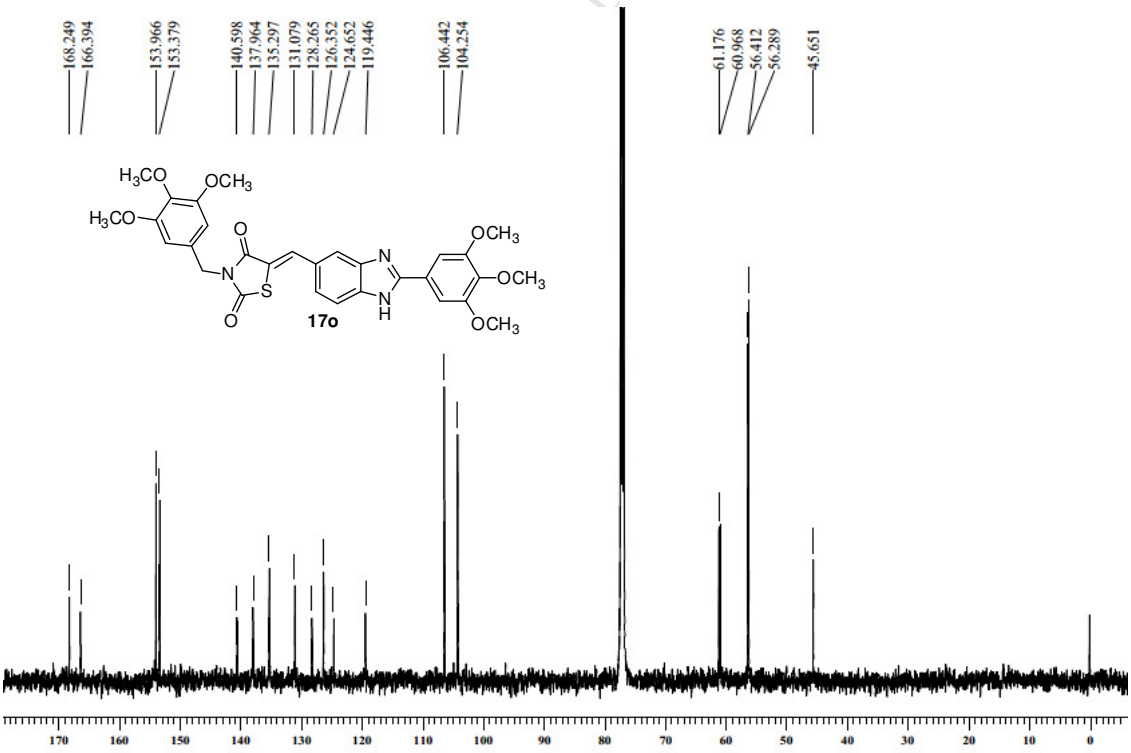

^{13}C NMR (125 MHz, $CDCl_3$) spectrum of compound **17o**

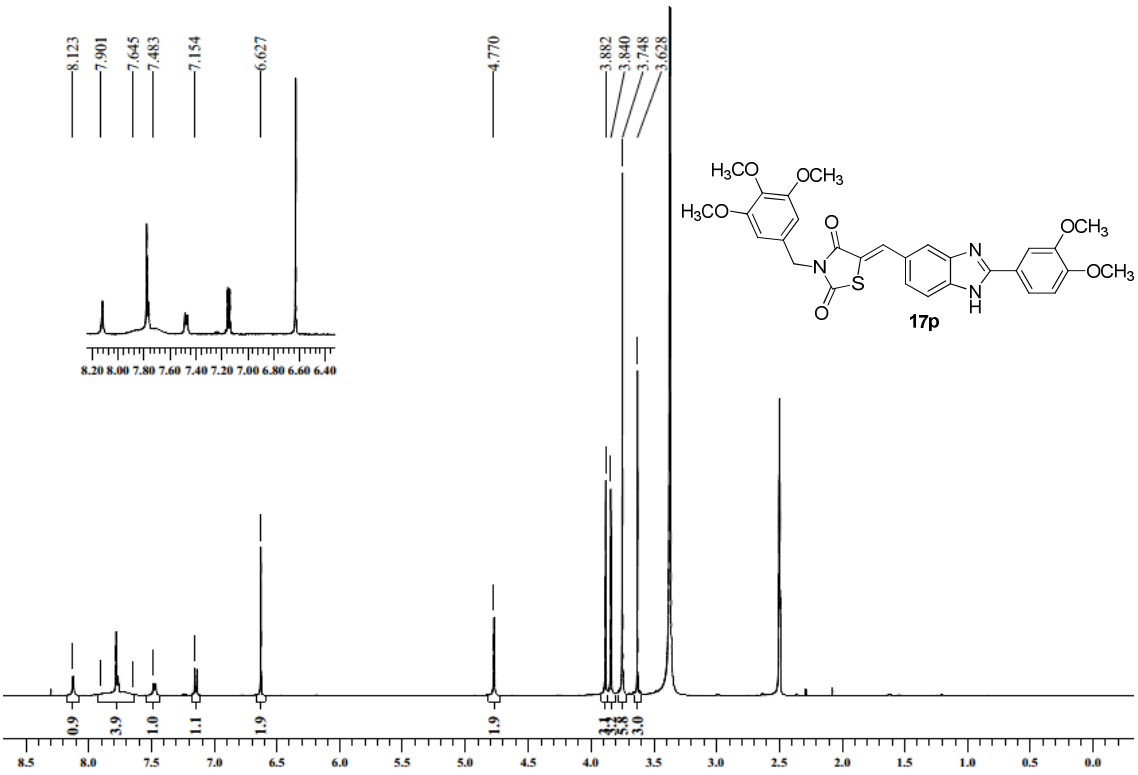

^{1}H NMR (500 MHz, DMSO-d_6) spectrum of compound **17p**

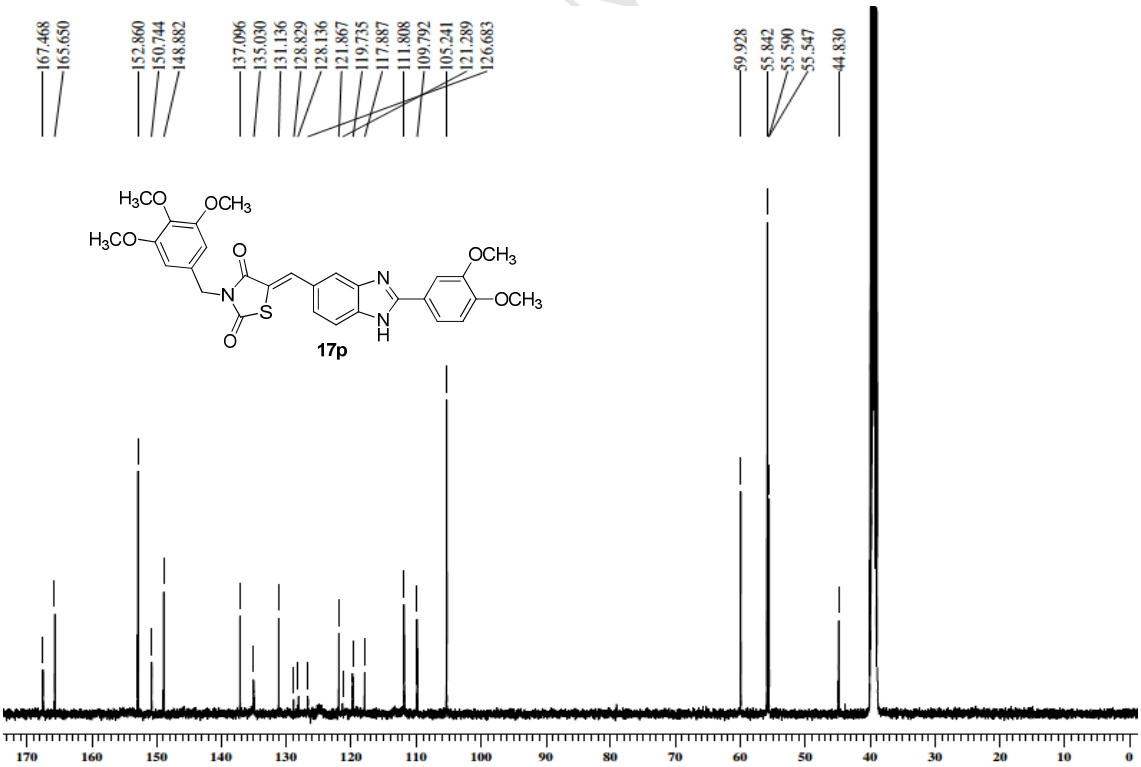

^{13}C NMR (125 MHz, DMSO-d_6) spectrum of compound **17p**

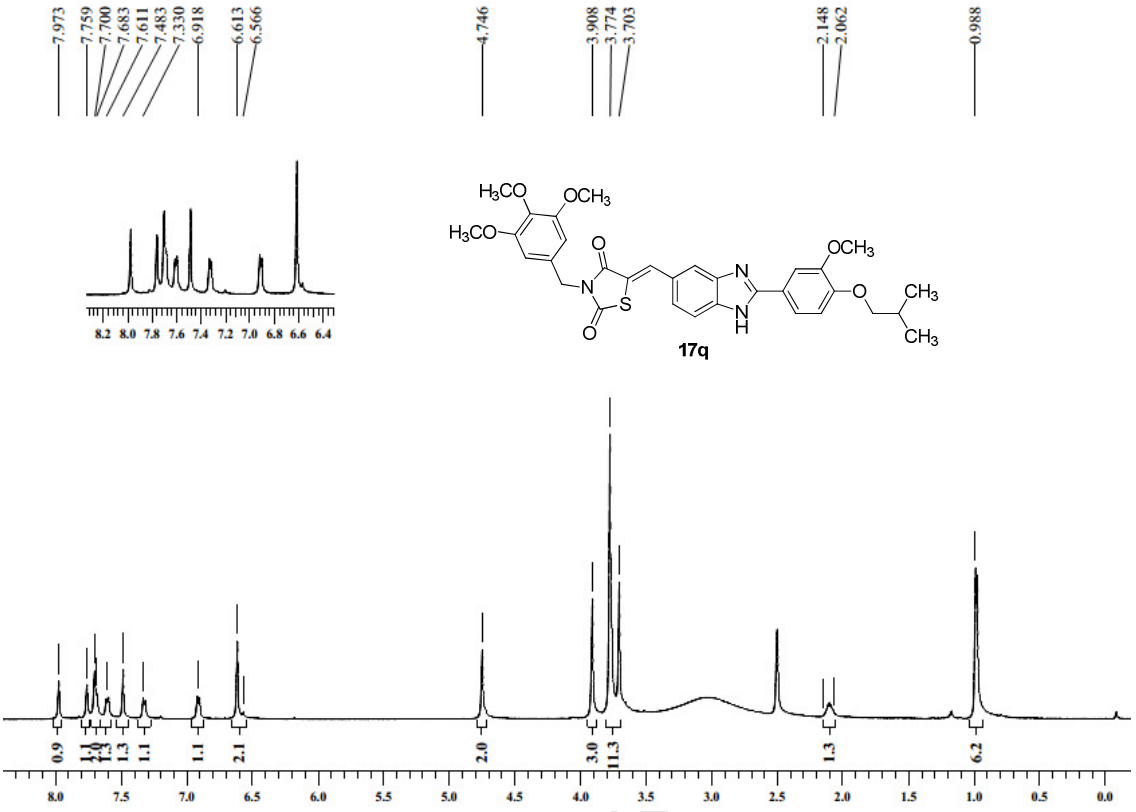

^{1}H NMR (500 MHz, $CDCl_3$+DMSO-d_6) spectrum of compound **17q**

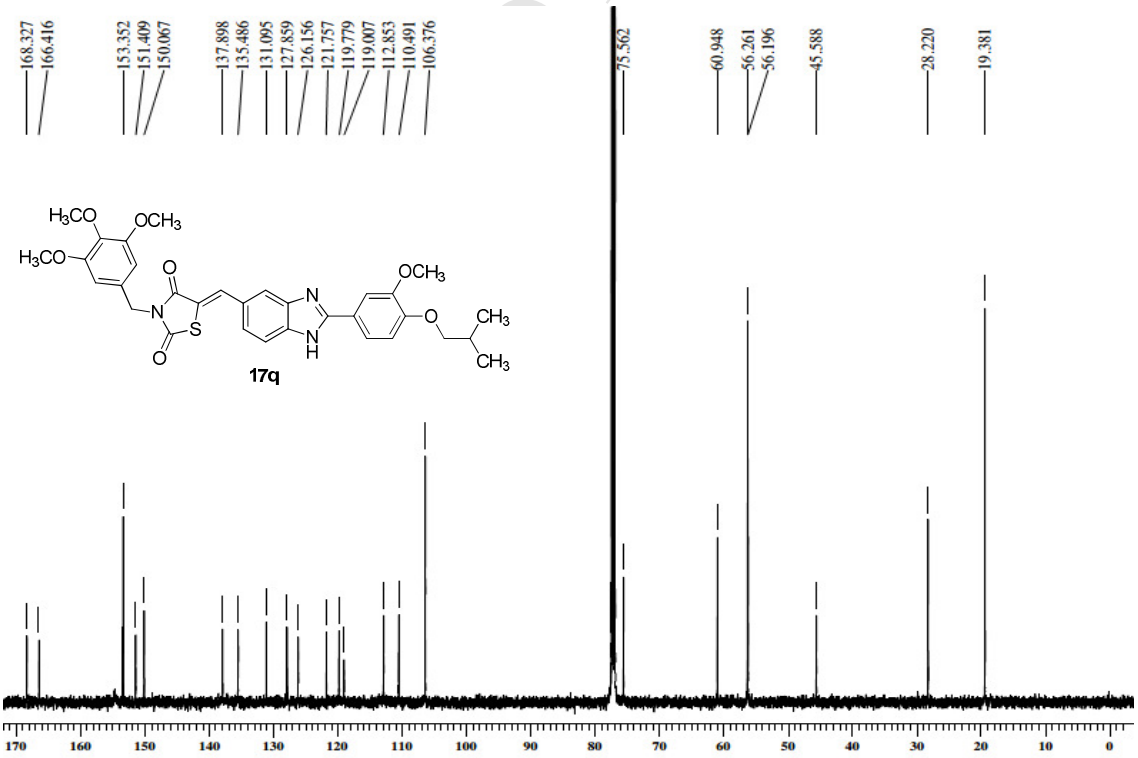

^{13}C NMR (125 MHz, $CDCl_3$) spectrum of compound **17q**

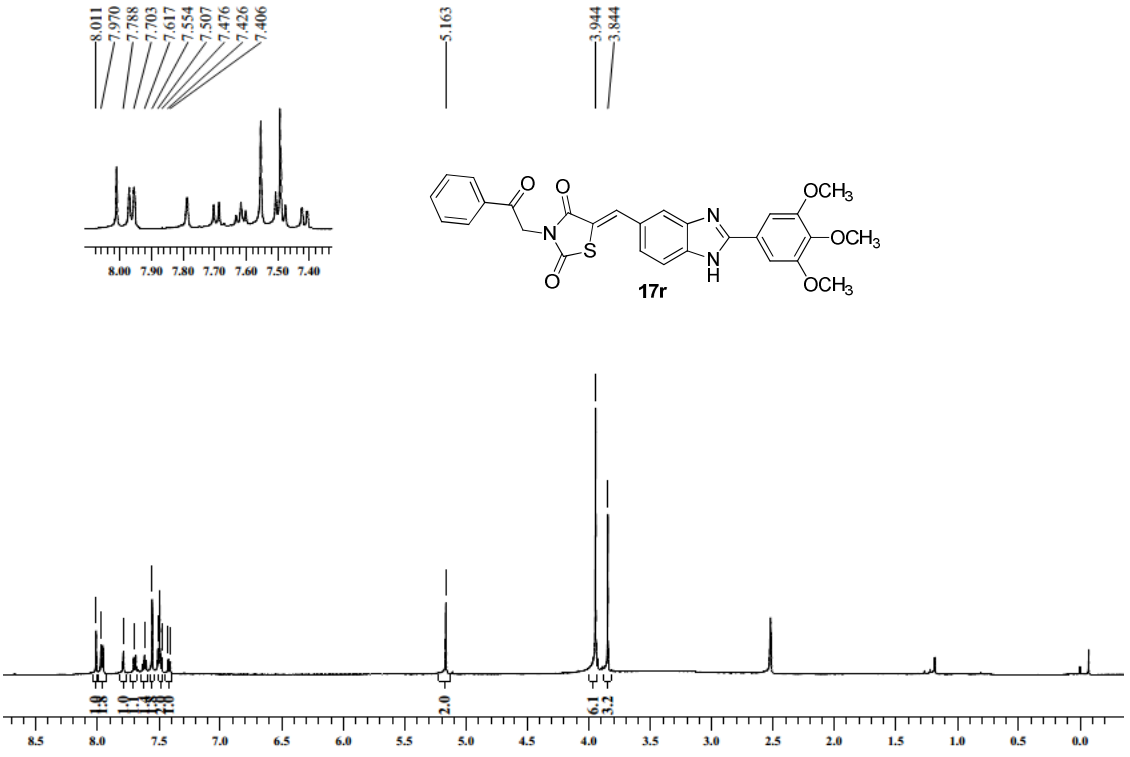

^{1}H NMR (500 MHz, $CDCl_3$+DMSO-d_6) spectrum of compound **17r**

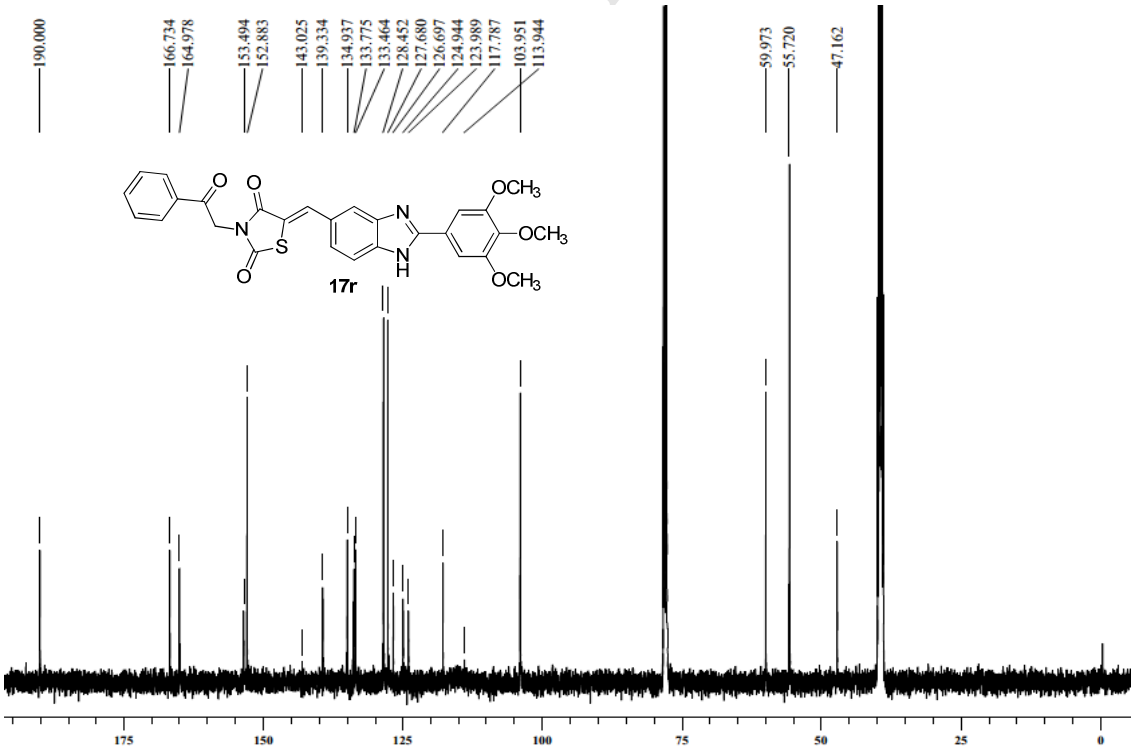

^{13}C NMR (125 MHz, $CDCl_3$+DMSO-d_6) spectrum of compound **17r**

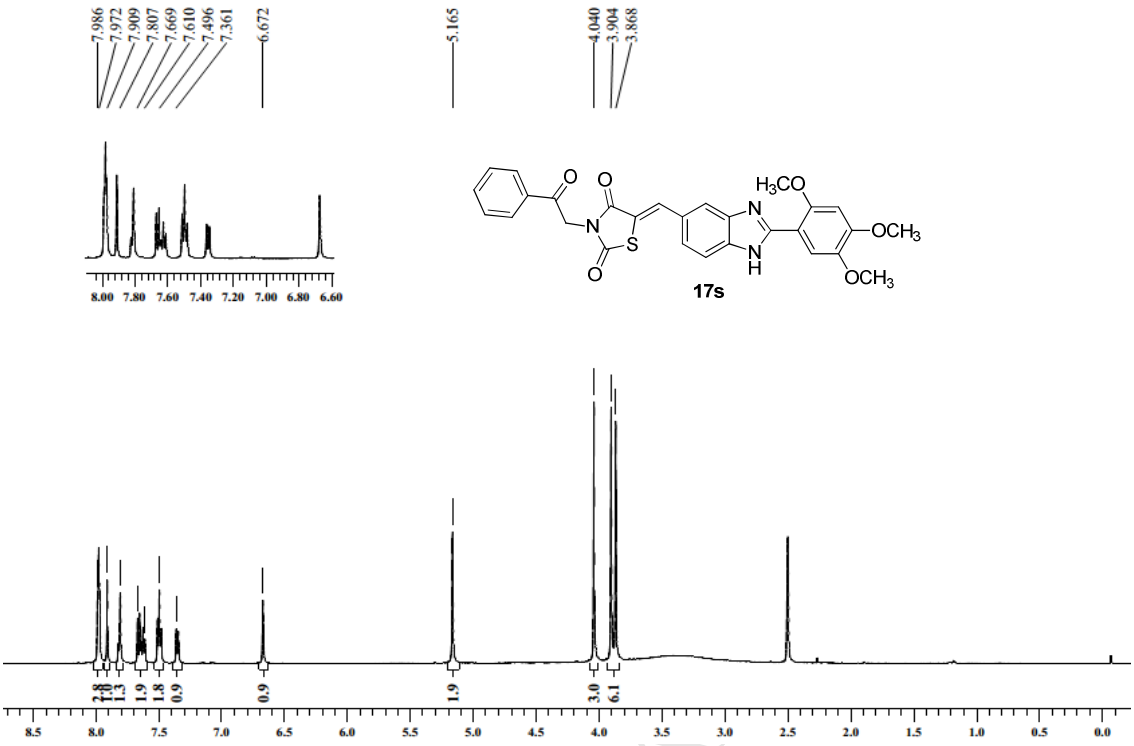

^{1}H NMR (500 MHz, $CDCl_3$+DMSO-d_6) spectrum of compound **17s**

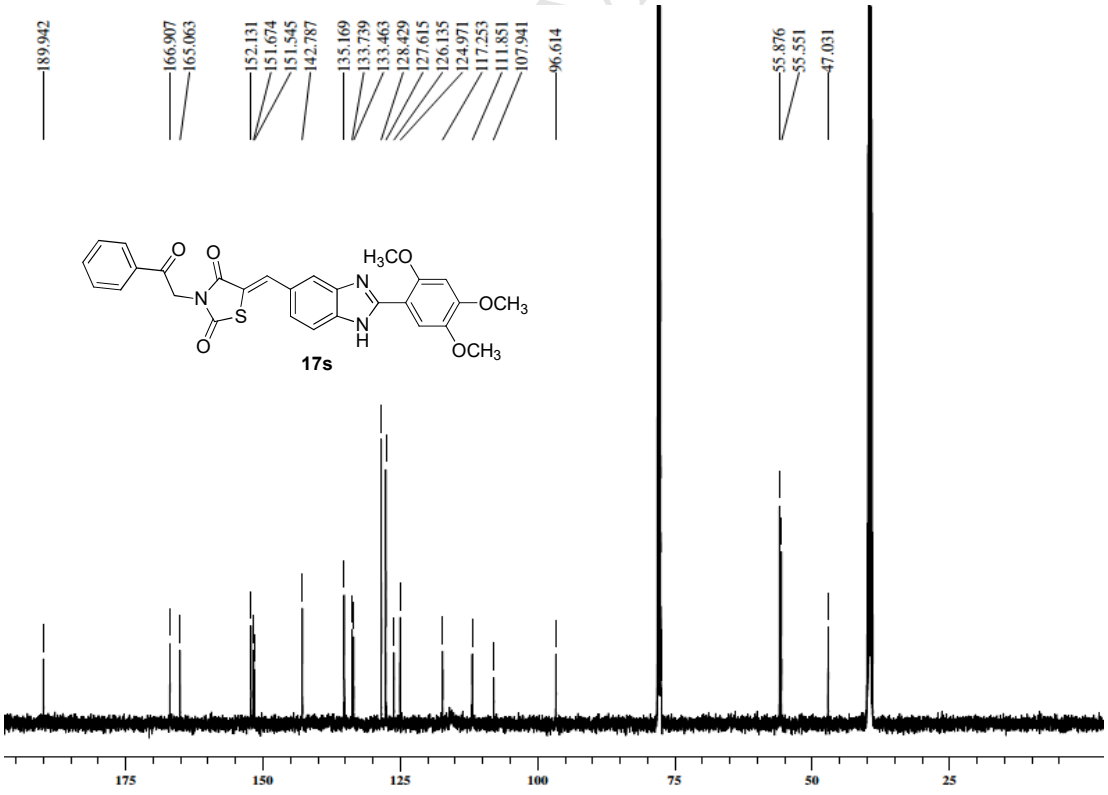

^{13}C NMR (125 MHz, $CDCl_3$+DMSO-d_6) spectrum of compound **17s**

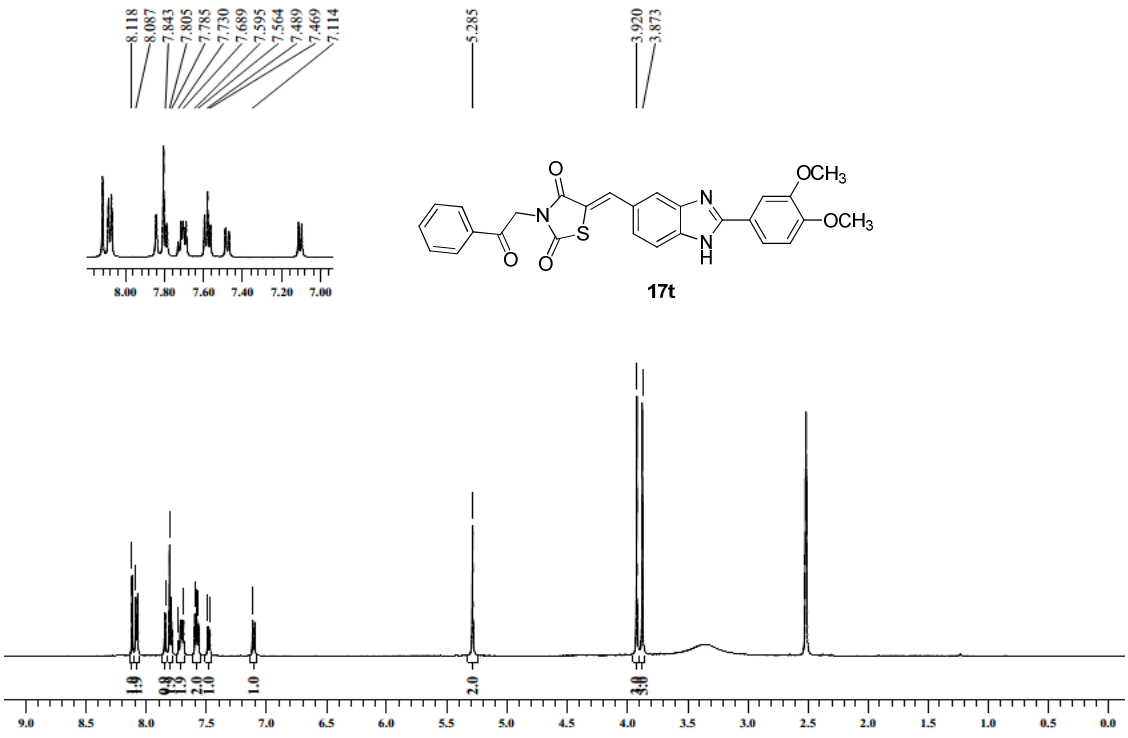

^{1}H NMR (500 MHz, $CDCl_3$+DMSO-d_6) spectrum of compound **17t**

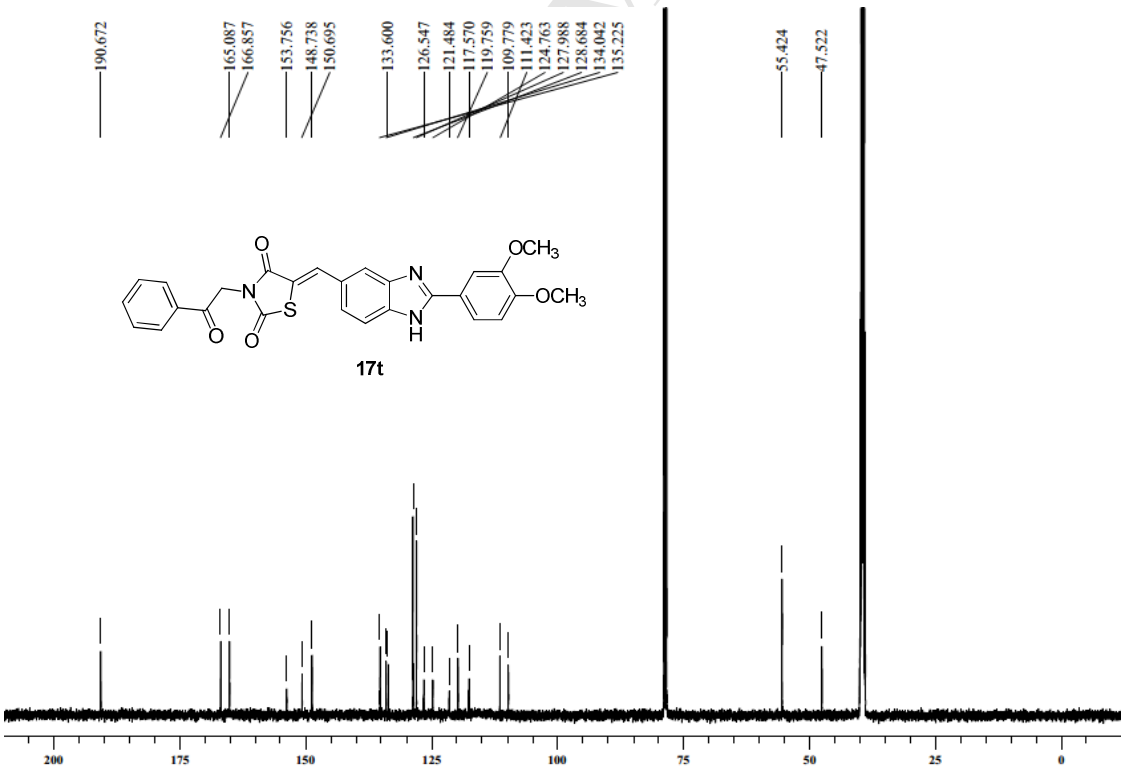

^{13}C NMR (125 MHz, $CDCl_3$+DMSO-d_6) spectrum of compound **17t**